IJCRT.ORG ISSN : 2320-2882

INTERNATIONAL JOURNAL OF CREATIVE RESEARCH THOUGHTS (IJCRT)

An International Open Access, Peer-reviewed, Refereed Journal

Importance And Advantages Of 1-D Tio_2 Photoanodes For Dye-Sensitized Solar Cell Applications

Kumar Vaisno Srivastava[1*], Raj Kumar Maurya[2], Yatendra Pal Singh[1]

[1]Department of Physics, Mangalayatan University, Aligarh-202146

[3]Department of Physics, Dr. RML Avadh University, Ayodhya-224001

Graphical Abstract

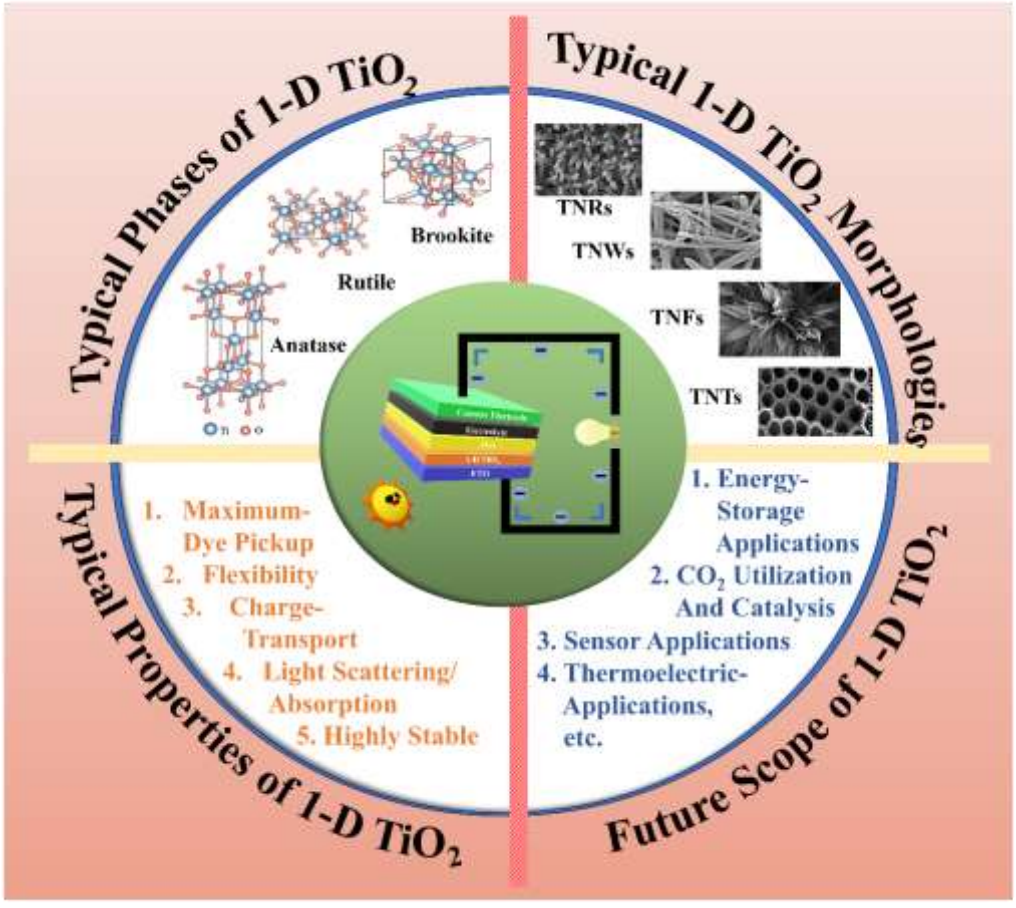

Schematic representing preliminary features, phases, nano-structures, and possible future applications of 1-D TiO_2 photoanodes.

Highlights

- Brief introduction of 1-D TiO_2 photoanodes and their role in DSSC.
- Demonstration of Typical TiO_2 phases and a variety of 1-D nanostructures such as nanorods, nanowires, nanotubes, etc.
- Successfully highlighted the importance and future scope of 1-D TiO_2 nanostructures in photovoltaics and beyond photovoltaics.

Abstract

Dye-sensitized solar cells (DSSCs) have emerged as a promising and sustainable alternative to traditional photovoltaic technologies. This study elucidates the pivotal role of one-dimensional titanium dioxide (1-D TiO_2) nanostructures as photoanodes in DSSCs. The distinctive morphology of 1-D TiO_2, including nanotubes or nanorods, provides an expanded surface area, facilitating efficient light absorption and dye adsorption. The inherent one-dimensional architecture promotes accelerated electron transport, minimizing recombination losses and enhancing charge collection efficiency. Additionally, 1-D TiO_2 structures exhibit superior charge carrier mobility, reducing trapping sites and enhancing electron diffusion pathways, thereby improving overall stability and performance. The scalability and cost-effectiveness of synthesizing 1-D TiO_2 nanostructures underscore their potential for large-scale DSSC production. This research emphasizes the significance of 1-D TiO_2 as a promising photoanode material, offering a pathway for advancing the efficiency and viability of dye-sensitized solar cell applications.

Keywords: Photovoltaics, Dye-Sensitized Solar Cell, 1-D TiO_2 photoanode, TiO_2-Nanorod, TiO_2-Nanowires, and TiO_2-Nanotubes.

1. Introduction

The excessive use of fossil fuels to meet our growing energy needs has resulted in significant consequences such as global warming and environmental pollution. To address these challenges and achieve a sustainable energy future, it is crucial to adopt an energy production approach that relies on renewable sources. While options like geothermal energy, biofuels, and wind-tidal energies can contribute to sustainable development, solar energy stands out as a particularly important solution. In this era of increasing energy demands and environmental concerns, solar radiation offers immense potential, abundant availability, and

environmental friendliness.[1] Out of the 4 million exajoules (1018 J) of solar energy reaching the Earth, approximately 50,000 EJ can be easily harnessed. The significance of solar energy is underscored by the fact that the world's annual energy consumption in 2017 amounted to approximately 565 exajoules (EJ), which represents a mere fraction of the potential solar energy harvest of around 50,000 EJ. However, the current contribution of the renewable energy sector to global electricity production stands at a modest 8.4%. Notably, solar energy accounts for over 20% of this renewable energy share.[2] Despite this, the utilization of solar energy remains disproportionately small compared to the vast solar power available for exploitation. The primary reason for this disparity lies in the absence of efficient and economically viable solar harvesting techniques. Among the diverse solar energy conversion devices, first-generation silicon solar cells have gained prominence as the most extensively commercialized type.

Silicon solar cells have achieved efficiencies of approximately 26%, approaching the theoretical maximum efficiency. In contrast, second-generation solar cells utilize thin-film technology and employ materials like CdTe and CIGS, reaching efficiencies of up to 21.7% in recent developments.[3][4][5] However, the widespread commercialization of first and second-generation solar cells remains costly, and the materials used in these generations can pose environmental hazards. To address these challenges and create an economically viable and environmentally friendly approach to solar energy conversion, the concept of dye-sensitized solar cells (DSSCs) was introduced as the third generation of solar cells. DSSCs, first proposed by Michael Grätzel in 1991, have garnered significant attention due to their potential for large-scale and cost-effective production, as well as their flexibility.[6] Currently, the efficiencies of DSSCs are within the range of 14.3%.[7] DSSCs have the potential to play a crucial role in advancing sustainable energy culture if the challenges of low efficiency and limited durability are effectively addressed. The large-scale commercialization of DSSCs can harness a significant portion of the available solar radiation. Enhancing performance, improving durability, and reducing production costs of DSSCs can be achieved through various approaches. This involves the synthesis of novel component materials or modifications to existing materials, as well as the introduction of more optimized DSSC designs. As DSSC assemblies consist of multiple components such as the photoanode, sensitizer (dye), counter electrode, and redox electrolyte, efforts to enhance performance can be focused on any of these components.[8] This review specifically highlights the significance of 1-D TiO_2 nanorods-based photoanodes for the critical advancement of DSSCs.

2. Fundamentals of DSSC

2.1. Architecture

Generally, DSSCs are composed of several key components that work together to convert sunlight into electricity. The architecture of a typical DSSC (shown in **Figure 1**) can be described as follows:

(i) **Transparent Conductive Substrate:** The DSSC starts with a transparent conductive substrate, commonly made of glass or a transparent conductive oxide (TCO) material like fluorine-doped tin oxide (FTO) or indium tin oxide (ITO). This substrate allows light to pass through and serves as the bottom electrode.

(ii) **Photoanode:** The photoanode is a thin layer coated on the conductive substrate and is usually made of nano-porous TiO_2 particles. These particles provide a large surface area for dye absorption and facilitate efficient charge transport.

(iii) **Sensitizer (Dye):** The sensitizer, or dye, is responsible for absorbing light and initiating the charge separation process. It is typically a light-absorbing organic dye or a dye-sensitized semiconductor material, such as ruthenium-based or organic dyes. The dye is adsorbed onto the surface of the TiO_2 particles, where it captures photons and transfers electrons to the TiO_2.

(iv) **Electrolyte:** The electrolyte plays a crucial role in DSSCs by facilitating the movement of charge carriers. In most DSSCs, a liquid electrolyte is used, containing a redox couple (typically iodide/triiodide) dissolved in a solvent. This redox couple shuttles electrons between the photoanode and the counter electrode.

(v) **Counter Electrode:** The counter electrode is usually made of a conductive material, such as platinum (Pt) or a carbon-based material like graphite. It acts as the cathode in the DSSC and catalyzes the reduction reaction of the redox couple from the electrolyte.

(vi) **Conductive Collecting Layer:** A conductive collecting layer is placed on top of the counter electrode to facilitate the collection of electrons and complete the circuit. It is often made of a transparent conductive material like FTO or ITO.

(vii) **Sealing:** To protect the sensitive components of the DSSC from moisture and environmental factors, the cell is sealed using a sealing material or encapsulation technique, such as a glass cover or a polymer layer.

When sunlight reaches the DSSC, it passes through the transparent conductive substrate and reaches the dye-sensitized TiO_2 particles in the photoanode. The dye absorbs photons and initiates the excitation of electrons, which are injected into the TiO_2, creating a flow of electrons through the photoanode. The electrolyte facilitates the movement of these electrons to the counter electrode, while the redox couple in the electrolyte is reduced. At the counter electrode, the electrons combine with the oxidized redox species, completing the circuit and generating an electric current. The unique architecture of DSSCs allows for efficient light absorption, charge separation, and collection, making them a promising technology for solar energy conversion. Ongoing research aims to optimize the architecture, explore new materials, and enhance the overall performance and stability of DSSCs.[9][10]

2.2. Electrical modelling

2.3. Working Principal

The working principle of a dye-sensitized solar cell (DSSC) involves several key steps that enable the conversion of sunlight into electrical energy. A schematic of DSSC fabrication and working mechanism is shown in **Figure 1**. The characteristic processes involved in DSSC working can be described as follows:

(i) **Light Absorption:** When sunlight reaches the DSSC, it encounters the photoanode, which consists of a thin layer of nano-porous TiO_2 particles. These TiO_2 particles have a large surface area, providing ample space for light absorption. The dye molecules, also known as sensitizers, are adsorbed onto the surface of the TiO_2 particles. The sensitizer absorbs photons from the incoming light, causing an electron within the dye molecule to be excited to a higher energy state.[11]

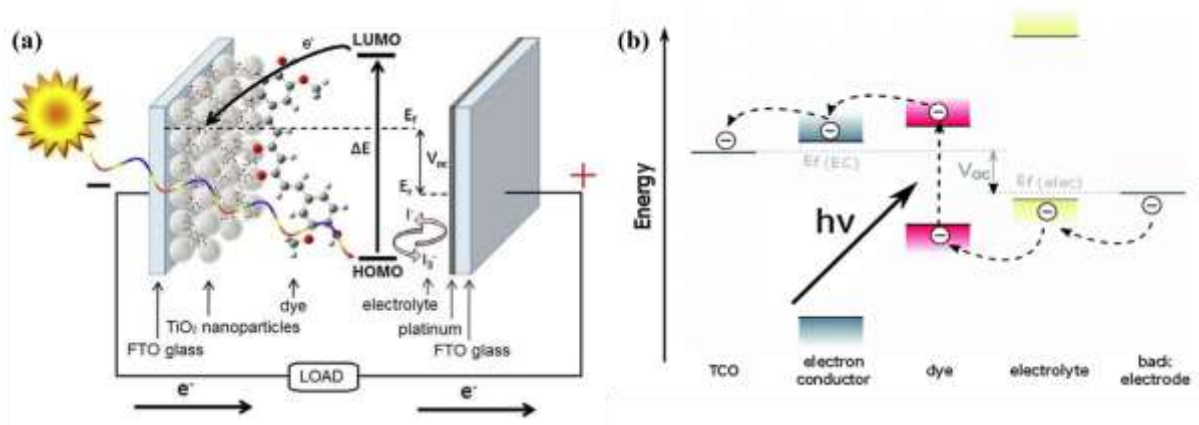

Figure 1. (a) Schematic assembly of DSSC and typical working mechanism,[12] (b) typical band alignment of DSSC.

(ii) **Electron Injection:** Once the sensitizer absorbs a photon and its electron is excited, the excited electron is injected from the sensitizer into the conduction band of the TiO_2 semiconductor. This process is facilitated by the favorable energy level alignment between the excited state of the dye and the conduction band of the TiO_2. The injected electron creates a mobile charge carrier within the TiO_2.[13]

(iii) **Charge Separation:** The injected electron in the TiO_2 travels through the nano-porous network, which allows for efficient charge transport due to the short diffusion paths. At the same time, the sensitizer molecule, after donating its electron to the TiO_2, becomes oxidized and positively charged. This charge separation creates a negatively charged region (electron-rich) in the TiO_2 and a positively charged region (hole-rich) in the sensitizer.[14]

(iv) **Electrolyte Redox Reactions:** To complete the circuit and maintain charge balance, an electrolyte is used in DSSCs. The electrolyte consists of a redox couple, typically iodide/triiodide (I^-/I_3^-), dissolved in a solvent. The I^-/I_3^- couple shuttles between the photoanode and the counter electrode. The triiodide (I_3^-) species in the electrolyte is reduced to iodide (I^-) at the photoanode, accepting electrons from the TiO_2 and regenerating the sensitizer. Meanwhile, at the counter electrode, iodide ions (I^-) are oxidized back to triiodide (I_3^-) species, completing the redox reaction.[15]

(v) **Electron Collection and Current Generation:** The electrons generated in the TiO_2 travel through a conductive collecting layer and reach the counter electrode, which is typically made of a conductive material such as platinum (Pt). At the counter electrode, the electrons combine with the triiodide ions (I_3^-) from the electrolyte, completing the circuit and generating an electric current. The counter electrode serves as the cathode, catalyzing the reduction reaction of the triiodide species.[16]

By continuously absorbing sunlight, initiating charge separation, and facilitating charge collection and regeneration of the sensitizer through redox reactions, DSSCs are able to generate a continuous flow of electric current. The efficiency of DSSCs is influenced by various factors, including the properties of the sensitizer, the design of the photoanode and counter electrode, and the efficiency of light absorption and charge transport within the cell. Ongoing research focuses on improving these aspects to enhance the overall performance and stability of DSSCs.

2.4. Important Parameters

DSSCs are characterized by several important parameters that determine their performance. These parameters include incident photon-to-current efficiency (IPCE), open-circuit voltage (V_{OC}), short-circuit current (J_{SC}), fill factor (FF), and overall cell efficiency. Each of these parameters plays a crucial role in the functioning and effectiveness of DSSCs.[3],[17],[18],[19]

2.4.1. Short-Circuit Current Density (J_{SC})

Figure 2 illustrates the current-voltage characteristics of a solar cell circuit under two conditions: in the dark and under illumination.[20] In the absence of illumination, when the electrons traverse from the anode to the cathode, or when the circuit is subjected to reverse bias, no current will flow due to the significant energy barrier presented by the donor material. Only after overcoming this energy barrier, a minimal current will be observed. This behaviour is depicted by the dark curve. Conversely, when the solar radiation is absorbed by the donor material, the generation of charge carriers becomes more facile. As a result, a reverse current occurs, where electrons flow from the anode to the cathode. This reverse current, in the absence of an external voltage, is referred to as the J_{SC}. This phenomenon is represented by the hollow bubbled curve. In summary, the current-voltage characteristics of the solar cell exhibit distinct behaviours under dark and illuminated conditions, reflecting the hindrance posed by the energy barrier in the absence of illumination and the enhanced generation of charge carriers in the presence of solar radiation.

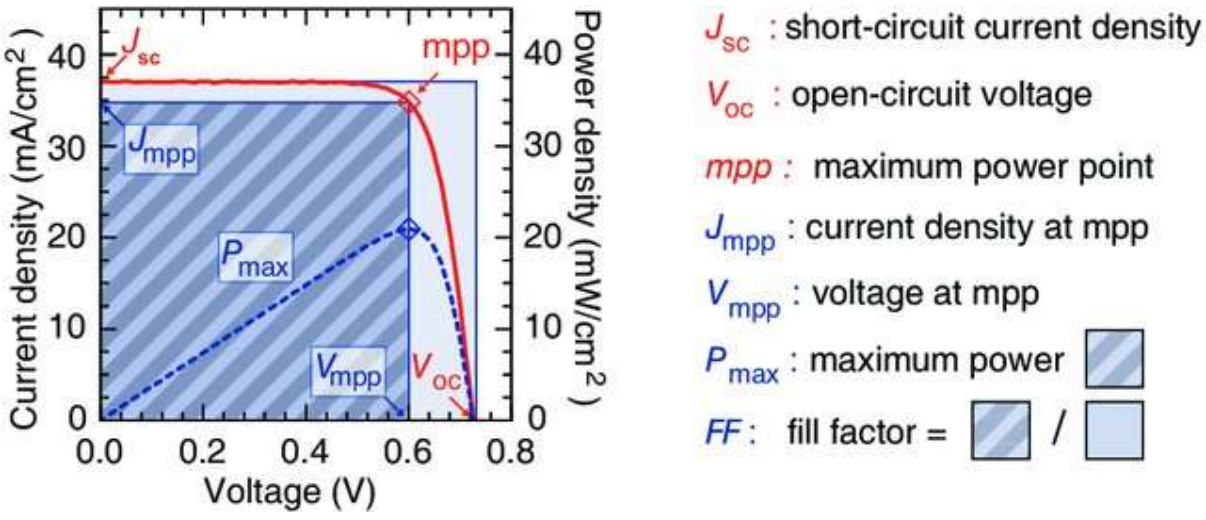

Figure 2. Typical schematic representation of various J-V parameters to evaluate the Solar Cell performance.[20]

2.4.2. Open-Circuit Voltage (V_{OC})

By applying a forward voltage to the solar cell, it is feasible to counteract the short circuit current, effectively compensating for its flow. This compensation process continues until a specific voltage is reached, at which point the current diminishes to zero. This specific voltage is termed the V_{OC}. On the other hand, the open circuit voltage represents the maximum attainable voltage across the terminals of a solar cell when it is not connected to an external load. In this state, no external current is drawn from the cell, and it operates under zero current conditions. The open circuit voltage serves as an indicator of the cell's inherent potential for generating electric energy without any external load connected.

2.4.3. Fill Factor (FF)

The FF of a solar cell provides an indication of its performance by comparing the actual power output to the maximum theoretical power output. It is calculated as the ratio of these two values.

$$FF = \frac{J_{mpp} \times V_{mpp}}{J_{SC} \times V_{OC}}$$

A higher fill factor indicates a more favourable condition for achieving the maximum power output of the solar cell. The graphical representation of the fill factor, as depicted in **Figure 2**, illustrates the relationship between the output current, power, and voltage of the solar cell. It can be visually represented as the ratio of the area enclosed by the larger rectangle (pale green) to the area enclosed by the smaller rectangle (yellow).

2.4.4. Power Conversion- and Incident Photon Conversion- Efficiency

Solar cell efficiency is a measure of the proportion of incident solar power that is converted into electrical energy. The efficiency of a solar cell is influenced by factors such as the spectrum and intensity of the incident sunlight, as well as the temperature of the solar cell. To facilitate accurate comparisons between different devices, it is essential to carefully control the conditions under which efficiency is measured. For terrestrial solar cells, efficiency measurements are typically conducted under standardized conditions known as AM1.5, which represents the solar spectrum at an air mass of 1.5. Moreover, these measurements are performed at a temperature of 25 °C to maintain consistency. The maximum output power of a solar cell, denoted as Pmax, is determined by the product of the V_{OC}, the J_{SC}, and the FF. The efficiency (η) of a solar cell is then calculated using the following equation:

$$\eta = \frac{V_{OC} \times J_{SC} \times FF}{P_{in}}$$

Here, P_{in} represents the input power of the solar cell. By employing this formula, the efficiency of a solar cell can be accurately determined, accounting for the interplay between open circuit voltage, short circuit current, and fill factor. Additionally, the incident photon-to-current efficiency (IPCE), also referred to as quantum efficiency, quantifies the relationship between the photocurrent (expressed as an electron transfer rate) and the rate of incident photons (derived from the calibrated power of a light source) at different wavelengths. It serves as a measure of a device's ability to convert incident photons into electrical energy with respect to a specific wavelength. In essence, IPCE characterizes the efficiency of a device in utilizing incident photons for the generation of electrical current, considering the wavelength-dependent conversion process. It provides valuable insights into the device's performance and its effectiveness in converting light energy into usable electrical energy at various wavelengths.

3. Importance of Photoanodes in Energy Conversion

The photoanode is a critical component among the functional elements of a DSSC. The performance of a DSSC is significantly influenced by the choice of material and morphology employed for the photoanode. The photoanode fulfils several crucial functions, including dye absorption, electron injection, transportation, and collection, all of which have direct impacts on the photocurrent, photovoltage, and power conversion efficiency of the DSSC. To enhance the efficiency of DSSCs, ongoing research focuses on the exploration of novel materials for use as photoanodes, as well as the modification of existing materials to optimize their morphologies. Achieving improvements in these areas is essential for advancing the overall performance of DSSCs. In order to meet the requirements of an ideal photoanode, certain key factors need to be considered. These include:

i. The surface area of the photoanode plays a critical role in enabling a higher degree of dye molecule adsorption. This increased surface area facilitates greater absorption of dye molecules, leading to enhanced light harvesting capabilities (**Figure 3(*a-b*)**).[21][22]

ii. To ensure efficient electron injection from the dye to the external circuit through the photoanode, it is essential for the photoanode to exhibit higher electron transport rates. This characteristic enables

smooth and rapid transfer of electrons, facilitating effective utilization of the absorbed photon energy (**Figure 3(*c*)**).[23]

iii. The photoanode material should possess suitable band gap alignment with the energy levels of the sensitizer. This alignment ensures efficient energy transfer from the sensitizer to the photoanode, optimizing the overall performance of the DSSC (**Figure 3(*c*)**).[24]

iv. High resistance to photo corrosion is a crucial requirement for the photoanode material. This resistance ensures the long-term stability and durability of the DSSC under prolonged exposure to light and other environmental factors.[23]

v. Optimizing the pore size of the photoanode material is important for achieving better diffusion of dye molecules and the electrolyte. This optimization enables efficient mass transport within the DSSC, enhancing the overall performance.[25]

vi. The photoanode material should exhibit the ability to absorb or scatter sunlight effectively. This characteristic promotes improved performance of the dye, enhancing the light absorption and conversion efficiency of the DSSC (**Figure 3(*d*)**).[26]

vii. Lastly, establishing optimum contact between the photoanode material, dye molecules, and the conducting substrate is crucial. This contact ensures efficient charge transfer and facilitates the effective utilization of generated electrons, ultimately enhancing the overall performance of the DSSC.[27]

This review focuses on the significance of utilizing TiO_2 nanomaterials as photoanodes in DSSCs. It provides an overview of the distinctive photovoltaic properties of TiO_2 and explores key modifications that have been made to enhance its performance as a photoanode material in DSSCs. The review also presents a comprehensive summary of recent research conducted on TiO_2, particularly focusing on its one-dimensional morphologies and the various modifications employed to optimize its suitability as a photoanode material in DSSCs.

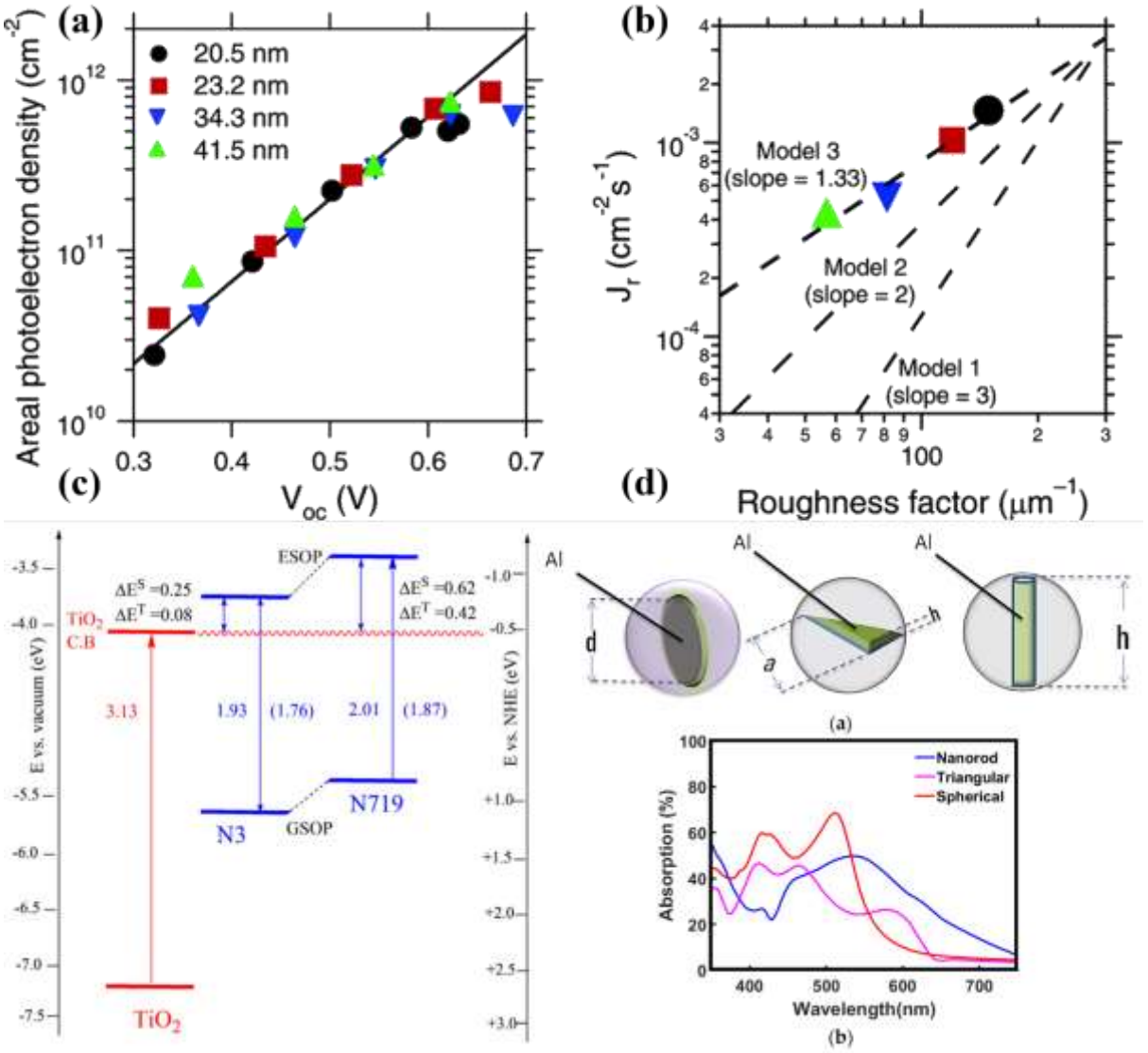

Figure 3. Important features of photoanodes that can affect the DSSC performance significantly (*a-b*) photoanodes surface area and roughness dependent photocurrent density,[21] (*c*) suitable bandgap alignment for better charge injection and transfer,[24] and (*d*) photoanodes morphology dependent tuning of light absorption capability causing enhanced performance.[26]

4. Classification of Photoanode Materials

Photoanode materials in DSSCs can be classified into several categories based on their composition and properties. Here are some common classifications of photoanode materials in DSSCs:

Metal Oxides: Metal oxides are the most widely used class of photoanode materials in DSSCs. TiO_2 is the most common and extensively studied metal oxide photoanode material due to its excellent stability, high electron mobility, and suitable band gap for efficient light absorption. Other metal oxides, such as ZnO, Fe_2O_3, Nb_2O_5, $SrTiO_3$, Zn_2SnO_4, and WO_3, have also been explored as photoanode materials in DSSCs. The photoanode materials used in DSSCs are typically wide band gap semiconductor materials. The performance

of DSSCs is heavily influenced by the structural, morphological, and crystalline characteristics of these materials. The band structures of these photoanode materials, which determine their electronic properties, can be observed in **Figure 4.**[28],[29],[30],[31] The specific arrangement of atoms and the overall crystal structure significantly impact the light absorption, charge transport, and electron injection processes within the DSSC, ultimately influencing its overall performance.[32],[33]

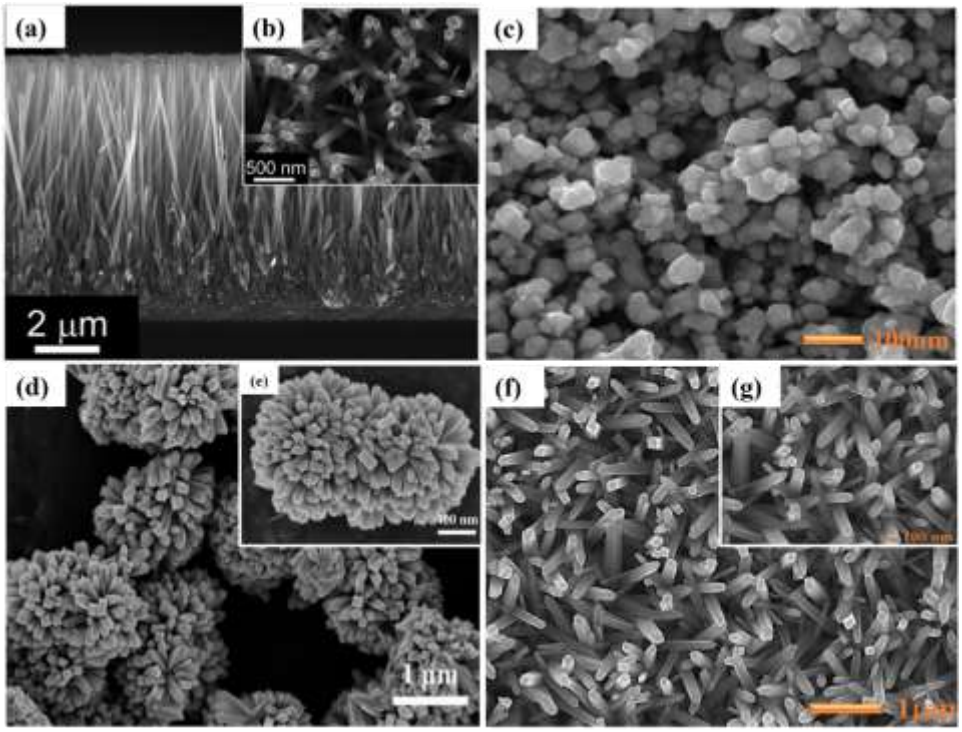

Figure 4. FESEM images of various metal oxides that were generally used as a photoanode in DSSC application. (*a-b*) ZnO-nanorods,[28] (*c*) Zn_2SnO_4-nanoparticles,[29] (*d-e*) SnO_2-nanoflower,[30] and (*f-g*) TiO_2-nanorods.[31]

Organic Semiconductors: Organic semiconductors have gained attention as photoanode materials in DSSCs due to their tunable optical and electrical properties. Materials such as conductive polymers (e.g., poly(3,4-ethylenedioxythiophene):poly(styrenesulfonate) (PEDOT:PSS)), phthalocyanines, and porphyrins have been investigated for their potential as photoanodes.[34]

Perovskites: Perovskite materials, particularly hybrid organic-inorganic lead halide perovskites (e.g., methylammonium lead iodide, $MAPbI_3$), have emerged as promising candidates for photoanode materials in DSSCs. Perovskites offer a high absorption coefficient, long carrier diffusion lengths, and tunable band gaps, making them attractive for efficient light harvesting.[35]

Nanomaterials: Various nanomaterials have been explored as photoanodes in DSSCs due to their unique properties and enhanced performance. These include nanowires, nanotubes, nanoparticles, and nanocomposites. Nanomaterials offer increased surface area, improved charge transport, and tailored optical properties, leading to enhanced device efficiency.[36]

Composite Materials: Composite photoanode materials, consisting of a combination of different components, have been investigated to synergistically combine the advantages of multiple materials. For example, composite photoanodes incorporating metal oxides, carbon-based materials (e.g., graphene), or organic semiconductors have been explored to enhance charge transfer, light absorption, and overall device performance.[37]

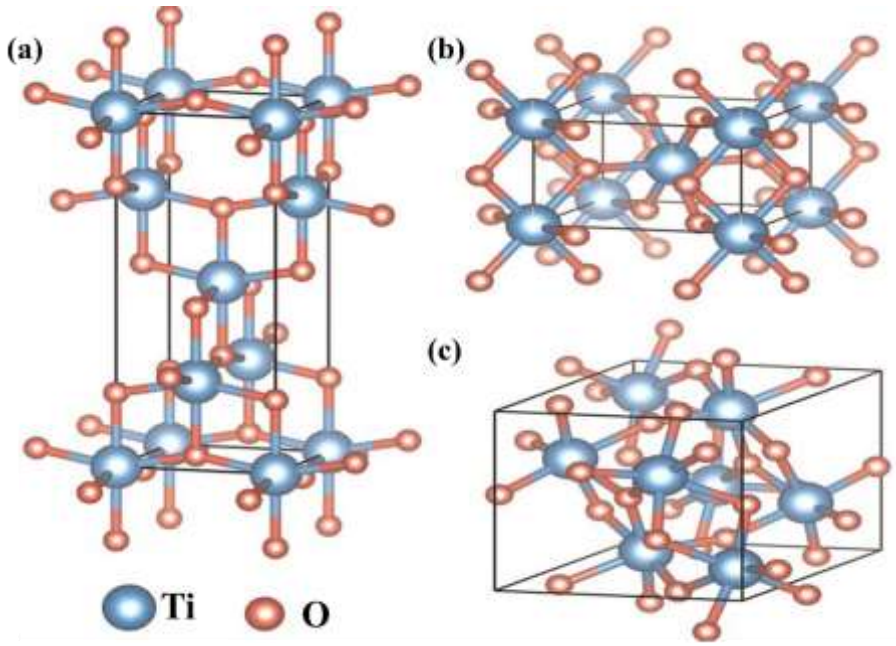

Figure 5. Typical ball-stick crystal structure of TiO_2 polymorphs. (*a*) anatase (tetragonal), (*b*) rutile (tetragonal), and (*c*) brookite (orthorhombic).[38]

It is worth noting that the classification of photoanode materials in DSSCs is not limited to these categories and continues to evolve as new materials and approaches are developed. TiO_2 and ZnO are widely utilized materials in the fabrication of DSSCs, with TiO_2 being the preferred choice due to its superior photovoltaic applicability compared to ZnO. Despite ZnO exhibiting higher electron mobility than TiO_2, DSSCs employing TiO_2 typically achieve higher efficiencies. This disparity in efficiency arises from ZnO's reduced dye adsorption capacity and its instability in acidic environments. TiO_2 exists in four known polymorphs: rutile (tetragonal), anatase (tetragonal), brookite (orthorhombic), and TiO_2 (B) (monoclinic), as

illustrated in **Figure 5.** Among these polymorphs, anatase is favoured over rutile for photovoltaic applications, despite rutile's greater stability and lower band gap. This preference stems from anatase's higher conduction band energy level, stronger light absorption characteristics, and lower electron-hole recombination rate. The synthesis of brookite TiO_2 poses challenges, making it less explored and less applicable as a photoanode material in DSSCs.[38]

DSSCs utilizing anatase TiO_2 have demonstrated efficiencies in the range of 12-14%. As a result, TiO_2 is considered the most favourable choice as a photoanode material due to its cost-effectiveness, easy availability, good stability, non-toxicity, and suitable optical and electronic characteristics. Moreover, many stable sensitizers, known for their high light absorption capability, exhibit a favourable alignment of their lowest unoccupied molecular orbital (LUMO) energy level with the conduction band of TiO_2. This alignment further enhances the performance of TiO_2 photoanodes. However, the use of TiO_2 as a photoanode material also presents challenges. Firstly, TiO_2 has a relatively large band gap of 3.2 eV, which results in predominant absorption in the UV region.[39] Secondly, TiO_2 exhibits a low internal electron transport rate. To address these challenges and improve the functionality of TiO_2 photoanodes, research efforts have focused on various factors such as increasing the surface area, enhancing light scattering effects, improving interface quality, achieving fast electron mobility, and enhancing charge collection abilities. Furthermore, the physical, chemical, and optical properties of TiO_2 depend not only on its intrinsic electronic structure but also on its shape, size, porosity, pore size distribution, organization, and surface features. Exploring and optimizing these factors contribute to the overall performance enhancement of TiO_2 in DSSCs.[40]

Achieving a higher dye pickup by the photoanode material leads to an increase in electron and current density generation. To enhance dye adsorption capabilities, various nanostructures of semiconductor mesoporous TiO_2, including nanorods, nanotubes, nanowires, nanosheets, and other nanoarchitectures, have been extensively employed and investigated as shown in **Figure 6(*a-f*)**.

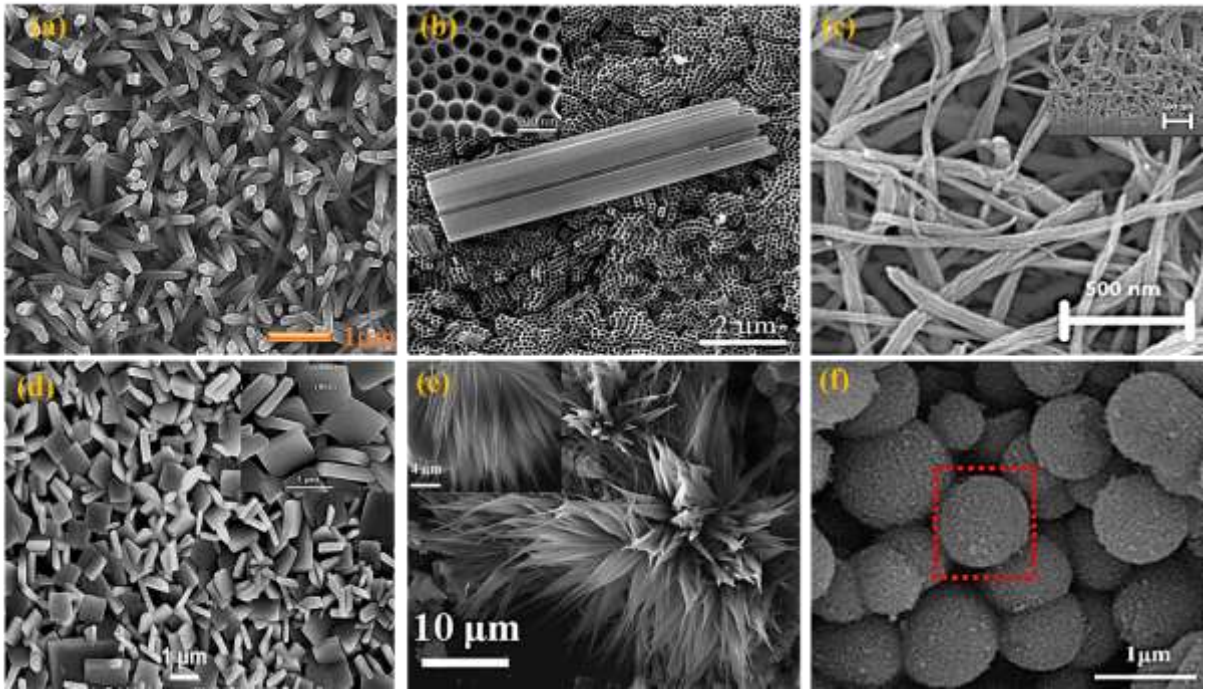

Figure 6. FESEM images of various TiO_2 photoanodes including 1D, 2D and 3D structures explored for DSSC application. (*a*) Nanorods,[31] (*b*) nanotubes,[41] (*c*) nanowires,[42] (*d*) nanosheets,[43] (e) nanoflower,[44] and (*f*) nanosphere.[45]

These nanostructures offer increased surface area, providing more binding sites for dye molecules and promoting efficient light absorption. In addition to maximizing surface area, enhancing electron mobility is crucial for improving photoanode performance. Defects present in TiO_2, particularly at grain boundaries, can act as electron traps, hampering the collection of injected electrons from the semiconductor. Therefore, minimizing or eliminating defects is essential to ensure efficient electron collection and transport within the photoanode material. Surface modification techniques have also proven effective in improving the performance of TiO_2 semiconductors. By modifying the surface properties, such as introducing surface coatings or functional groups, charge separation, electron mobility, and the recombination process can be significantly influenced. These surface modifications play a crucial role in facilitating efficient charge separation, reducing electron recombination, and improving overall photoanode performance in DSSCs.[41][42][43][44][45]

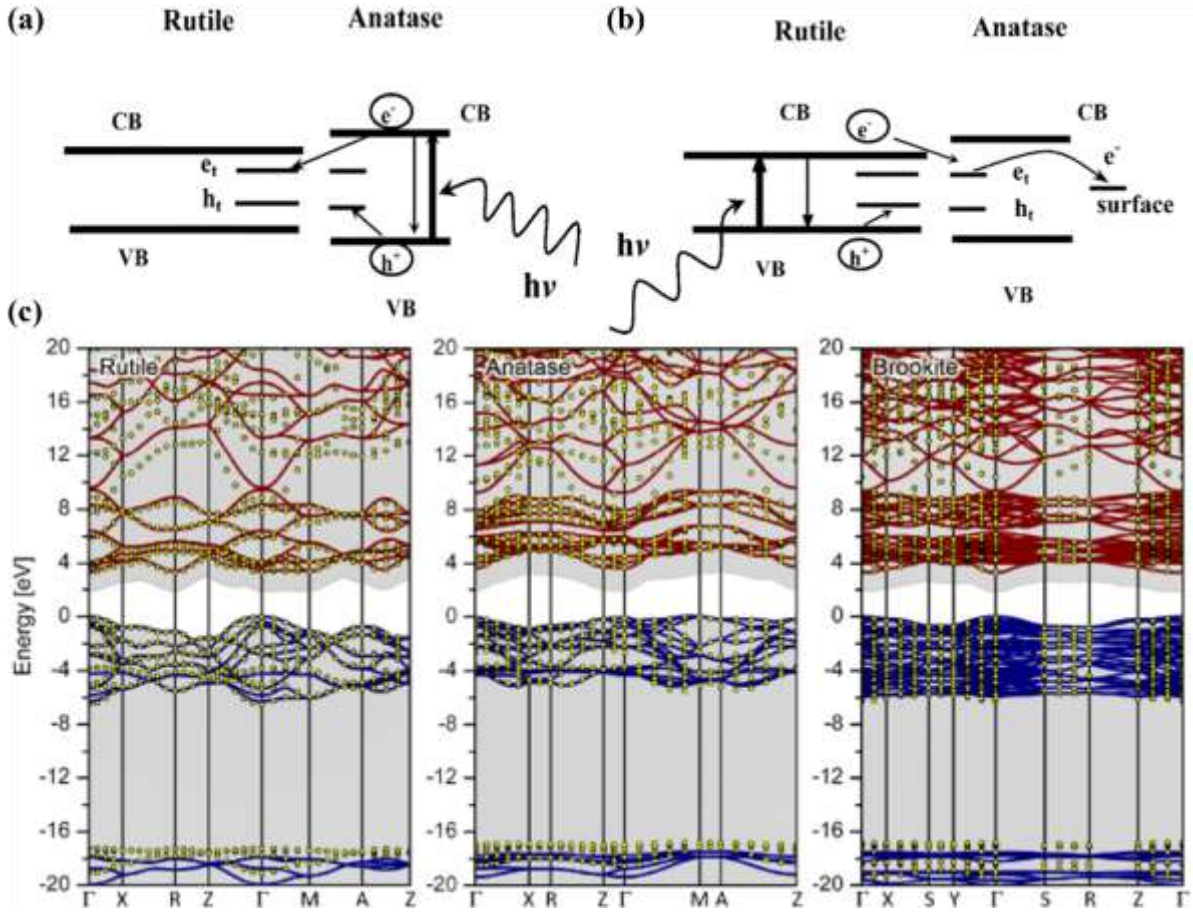

Figure 7. (*a-b*) Typical schematics of charge trapping process in two phase TiO_2 namely rutile and anatase which illustrating that photogenerated charges in anatase phase can further trapped via injection in rutile phase,[46] (c) Typical band-structures and quasi particle energies of different TiO_2 phases (-*Rutile*, -*Anatase*, -*Brookite*).[47]

Doping in the TiO_2 lattice can effectively modify its electronic properties through the intentional introduction of impurities. By incorporating dopants into the TiO_2 structure, the number of free charge carriers and the overall conductivity of the material can be increased. This phenomenon arises from the inherent presence of defects within the TiO_2 lattice, which directly influence the electronic structure and the occurrence of trap states within the material (**Figure 7**).[46][47] During the doping process, either the Ti^{4+} cations or the O^{2-} anions can be substituted with other atoms. Consequently, the replacement of Ti^{4+} cations or O^{2-} anions leads to alterations in the conduction band (CB) and valence band (VB) structures, respectively. The CB energy levels are primarily formed by the orbitals of Ti^{4+} ions, while the VB energy levels predominantly consist of the O^{2-} 2*p* orbitals (**Figure 8**).[48][49]

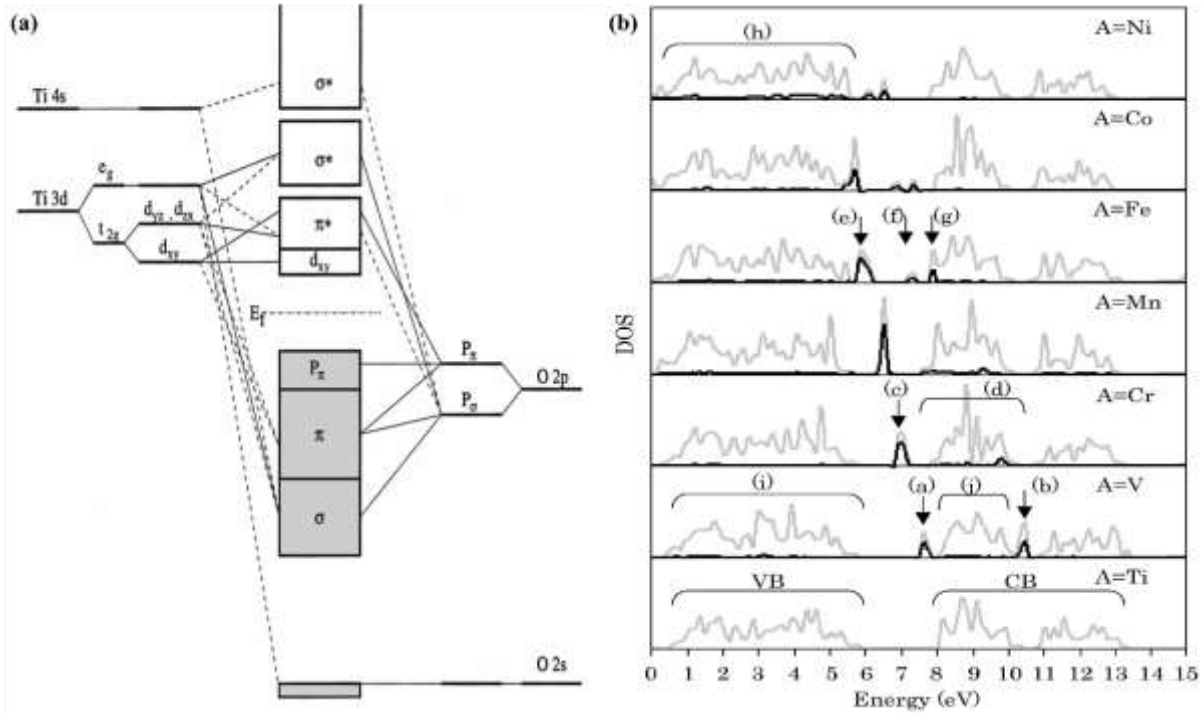

Figure 8. (*a*) Detailed molecular orbital bonding diagram of TiO_2 composed of the components extracted from the DOS spectra,[48] (*b*) Density of states (DOS) of $Ti_{1-x}A_xO_2$ doped via various metals (A: V, Cr, Mn, Fe, Co, Ni) where grey lines and black lines representing total DOS and dopant DOS respectively.[49]

Doping of TiO_2 nanoparticles has been observed to have a significant effect on their growth rate, resulting in the formation of smaller particles with a greater surface area compared to undoped TiO_2. This inhibition of growth can be attributed to the presence of dopant atoms within the TiO_2 lattice, which introduce defects and alter the crystal structure, thereby hindering the crystal growth process. The increased surface area of doped TiO_2 nanoparticles offers several advantages. Firstly, it enhances the adsorption capacity of dyes onto the TiO_2 surface, leading to improved performance in applications such as DSSCs. The larger surface area provides more active sites for the dye molecules to attach, promoting efficient light absorption and conversion.[50]

The optical and electronic properties of TiO_2 are significantly influenced by its various morphologies. It has been observed that one-dimensional nanostructures such as nanowires, nanorods, and nanotubes exhibit superior charge transport properties compared to assemblies of TiO_2 nanoparticles. However, these one-dimensional structures possess a smaller surface area than nanoparticle systems, resulting in reduced dye adsorption capability. To address this limitation, the introduction of dopants with enhanced dye adsorption capacities can improve the photovoltaic performance of one-dimensional nanostructures.[51] This allows for better utilization of incident light and improved conversion of photons into charge carriers. On the other hand,

nanoparticle assemblies can benefit from dopants that promote increased charge transfer processes. These dopants facilitate efficient electron transfer between the TiO_2 nanoparticles, enhancing the overall conductivity and charge transport within the material. As a result, it becomes challenging to determine the precise contribution of absorption enhancement or electronic effects in doped TiO_2 towards the improvement of its performance. Both factors, the increased absorption of light due to enhanced dye adsorption and the improved charge transfer properties resulting from dopants, play a crucial role in enhancing the overall photovoltaic performance of doped TiO_2 materials.[52]

Nanotubes, nanowires, nanofibers, nanobelts, and nanoribbons are a few examples of one-dimensional nanostructures that have found extensive use in DSSCs. The ground-breaking research by Iijima *et al.* is largely responsible for growing interest in these nanomaterials.[53] For electron transport from the semiconductor layer to the conducting substrate, their orderly alignment provides an identifiable route. This has two effects: first, it slows down the rate of electron recombination, and second, it improves the solar cell's efficacy.

4.1. 1-D Nanowires

In DSSCs, TiO_2 nanowire (TNW) architectures are significant because they function as constrained conducting channels with long charge diffusion lengths that efficiently avoid charge recombination and promote optimal charge transport. They are now considered to be potential candidates for use in the manufacture of DSSC due to their special characteristic. When used as dye scaffolds, a dense array of long, thin nanowires can dramatically improve both dye absorption and carrier collecting efficiency. Additionally, nanowire photoanodes show superior compatibility with unconventional electrolytes such solid inorganic phases or polymer gels, which normally have greater recombination rates (**Figure 9**).[54]

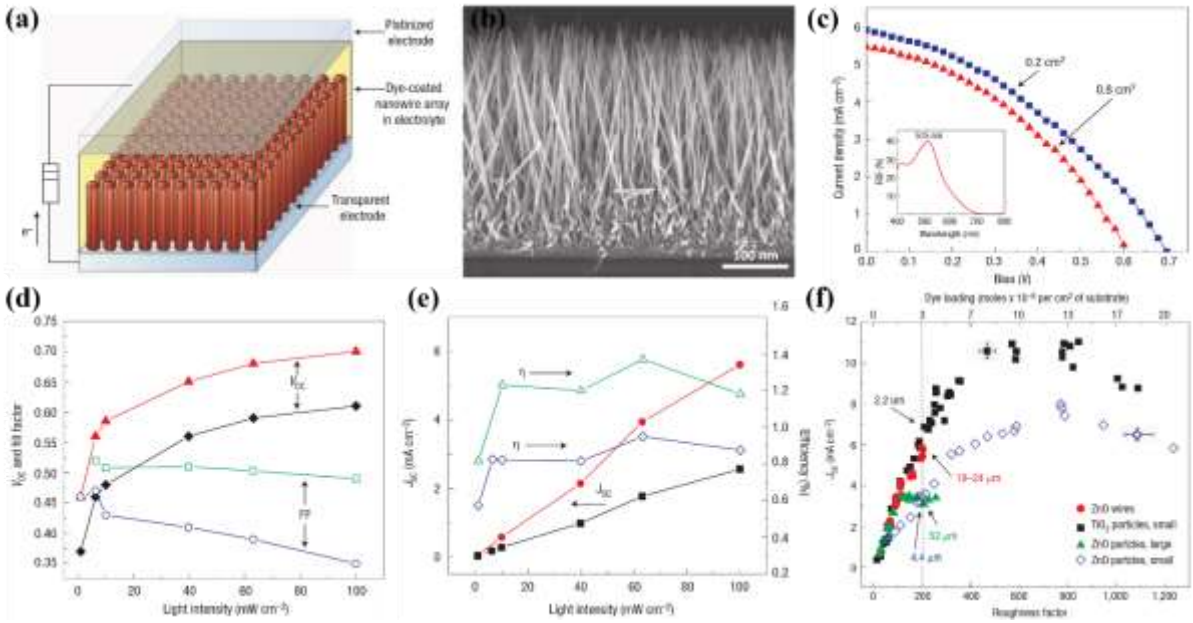

Figure 9. (*a*) Schematic DSSC fabricated using TiO_2 nanowires as a photoanode, (*b*) typical FESEM image of cross-sectional view of TiO_2 nanowires, (c) *J-V* analysis of respective DSSC with two different active area of 0.2cm^2 and 0.8cm^2 along with quantum efficiency curve shown inset, (*d-e*) Trace of V_{OC}, FF, J_{SC}, and η against light irradiance, (*f*) comparative analysis of DSSC prepared using nanoparticles and nanowires with respect to roughness and dye-loading.[54]

The electron-hole recombination time and electron collection time ratio of TNW-based DSSCs are exceptional, being around 150 times higher than those of nanoparticle-based solar cells. This substantial variation emphasises the higher collecting efficiency attained with nanowire arrays. The various initiatives made to improve the critical aspects affecting the overall efficiency of TNW-based DSSCs are summarised in **Figure 10**.[55]

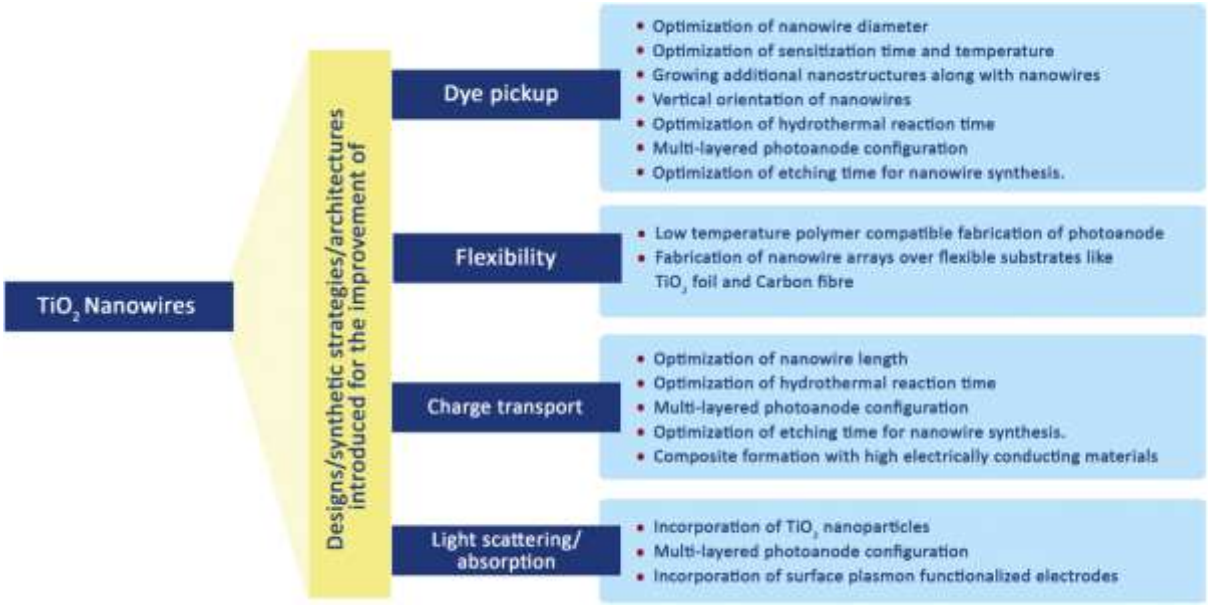

Figure 10. Various modifications made in TiO_2 nanowires to improve the DSSCs performance.[55]

Feng *et al.* introduced a simple technique for producing single-crystalline rutile TNWs at low temperatures. The method involves a nonpolar solvent and a hydrophilic solid substrate interfacial reaction under hydrothermal conditions. Using this approach, they were able to grow vertically aligned nanowires with lengths of up to 5 µm on TCO glass substrates. When N719 dye was applied to the TNW arrays measuring 2–3 µm in length, the system achieved an efficiency of 5.02% under AM1.5 irradiation.[56] Consequently, the implementation of low-temperature techniques for photoanode fabrication is compatible with polymer substrates, enabling enhanced flexibility in the process. A hydrothermal technique capable of precisely creating TNW arrays on a titanium mesh with an average diameter of 80 nm was presented by Liu *et al.* in 2015. The researchers focused on the effect of sensitization temperature and time on the performance of DSSCs, in addition to examining the effects of various TNW array preparation procedures on the parameters of DSSCs. They found that complete monolayer dye molecule coverage on the surface of the TNW arrays improved the photovoltaic characteristics of the DSSC, but higher sensitization temperatures permitted better infiltration of dye molecules into the internal regions of TNW array films. Liu *et al.* were successful in achieving an efficiency of 3.42% for a flexible DSSC by carefully preserving ideal circumstances and shown in **Figure 11(g-f)**.[57] Additionally, in addition to attaining the intended dye uptake, their method also effectively reduced charge recombination problems.

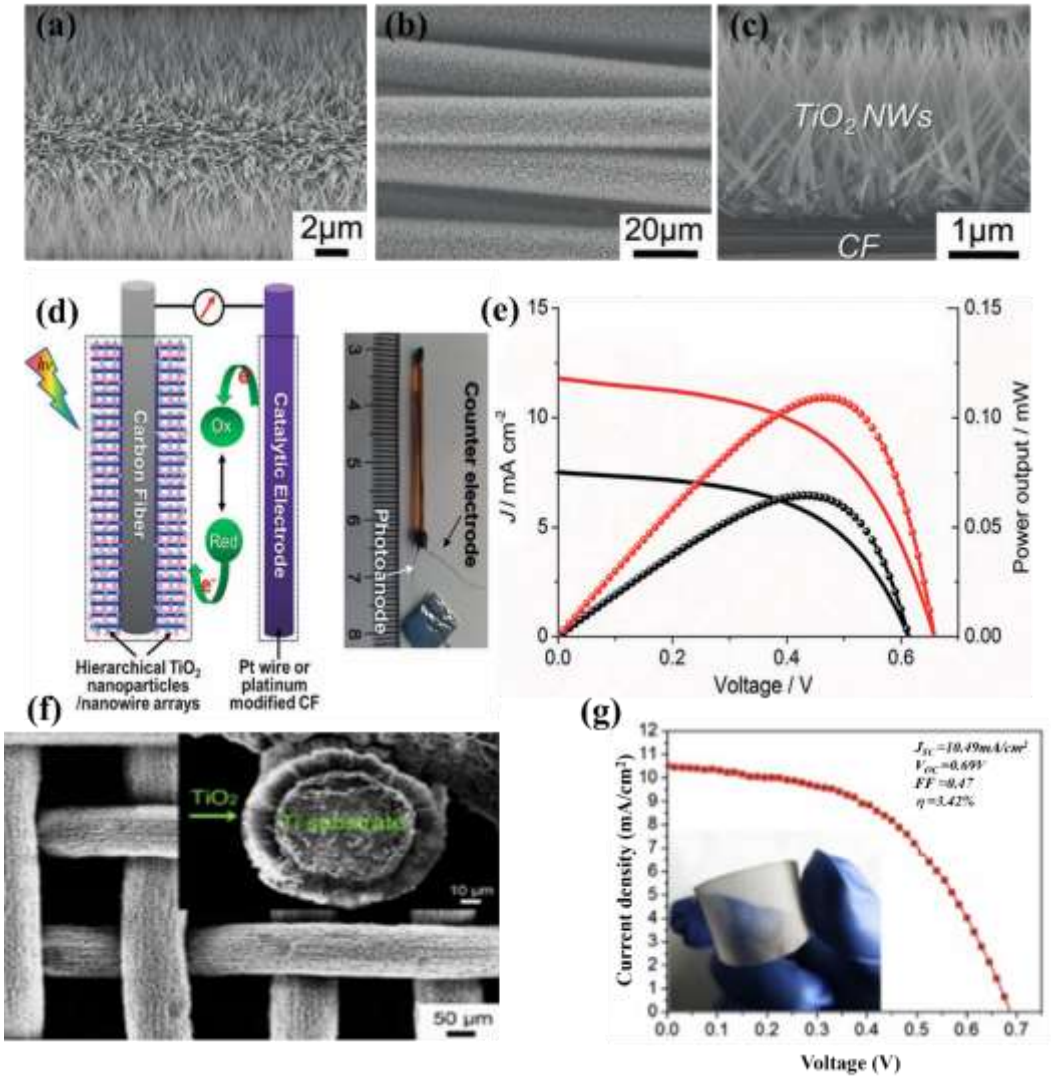

Figure 11. (*a-c*) FESEM images of hierarchical TiO_2 nanowire arrays grown over the CF substrate at 190°C for 80 minutes, (*d-e*) schematic of wire DSSC consisting TiO_2 nanoparticle and nanowires and Pt-modified CF counter electrodes and consequent *J-V* analysis, (f-g) Low-magnification FESEM images of the TiO_2 NWAs on Ti mesh substrates and respective *J-V* performance.[57]

In a unique TiO_2 structure described by a corn-like nanowire shape, Bakshayesh *et al.* used a surface tension stress mechanism to produce high surface area and crystallinity. For their DSSC, they used a double-layer design that included a bottom layer of anatase TiO_2 nanoparticles and a top layer of corn-like TNWs. Bakshayesh *et al.* attained a remarkable efficiency of 7.11% by using a triple-function mechanism that successfully controlled light scattering, dye sensitization, and efficient photogeneration of charge carriers. Corn-like nanowires' increased surface area considerably enhanced dye sensitization and J_{SC}, and the presence of nanoparticles on these nanowires improved the effects of light scattering, which helped to improve overall performance.[58] By using an 8-hour reaction period, Zha *et al.* produced 6 μm long nanowires with an efficiency of 5.61%. This emphasises how the microstructure has a substantial impact on the performance of

solar cells, and the DSBS structure shows considerable promise as a viable contender for increasing efficiency.[59] Then, Qiang Wu and his team created a DSSC that boasted a remarkable efficiency of 9.40% (**Figure 12**) using a self-assembled, vertically aligned TNWs photoelectrode sensitised using N719 (ref. 133) sensitizer. TNWs on an FTO glass plate are appropriate for use in multi-layered photoanode setups because they can be adjusted to varying lengths between 15 and 55 μm.[60]

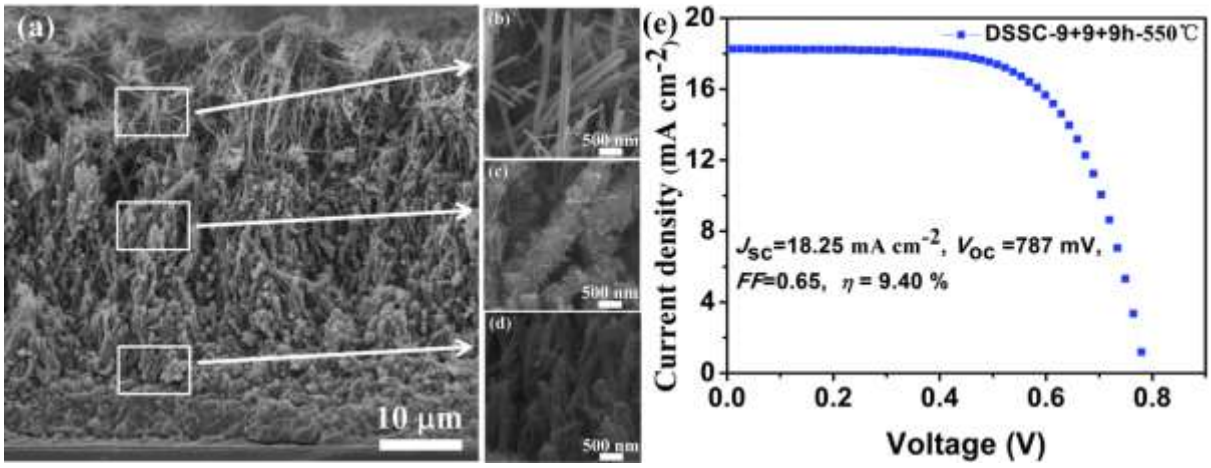

Figure 12. (*a*) Cross-sectional FESEM image of TiO_2 nanowires grown on FTO substrate in 3 cycles of 9 hr each, (*b-d*) FESEM images of Top, intermediate, and bottom layers of grown nanowires, (e) *J-V* analysis of the DSSC prepared using these TiO_2 nanowires having total thickness of 47μm.[60]

A unique DSSC created by Yen *et al.* successfully integrated plasmonic and antireflective properties. Their DSSC included a 3D TNW-AuNP plasmonic electrode made up of Au nanoparticles (NPs) attached to antireflective TNWs, which served as light-harvesting antennae. The absorption wavelength was increased from 520 nm to 575 nm as a result of the use of plasmonic functionalized electrodes (PFEs). This strategy intended to get beyond the drawbacks of standard DSSCs' small dye absorption ranges and poor dye absorption coefficients. $TiCl_4$ treatment was used to further improve the TNW-Au-NP hybrid DSSCs' efficiency, leading to a notable improvement from 6.25% to 9.73%. It was shown that combining antireflective qualities with plasmonic effects was a successful way to boost the efficiency of DSSC.[61]

In their study, Wu *et al.* established a distinctive and inventive architecture by integrating various three-dimensional, hyperbranched titania nanostructures in a multi-stack configuration. The photoanode design comprised of three layers: a bottom layer composed of hyperbranched hierarchical tree-like titania nanowires, an intermediate layer featuring branched hierarchical rambutan-like titania hollow sub-micro-meter-sized spheres, and a top layer encompassing hyperbranched hierarchical urchin-like titania micro-

meter-sized spheres. Each layer had a distinct function that improved the photoanode's overall performance. Efficient electron transport from 1-D nanowires to the FTO plate was made possible by the bottom layer. Due to the hollow-hole structure of the sub-micro-meter-sized macro-porous TiO_2 spheres, the intermediate layer provided excellent light-trapping efficiency. On the other hand, more light might be scattered thanks to the higher layer of hyperbranched hierarchical TiO_2 microspheres. The combination of these various nanoarchitectures produced an astounding photoanode efficiency of 11.01%, outperforming its TiO_2 nanoparticle counterpart appreciably.[62] The creation of outstanding performance photoelectrochemical devices for a variety of applications is greatly enhanced by this research. The previous discussion highlighted the substantial endeavours undertaken to enhance the performance of nanowire-based DSSCs, and a summary of these efforts is provided in **Table 1.**

Table 1. Comparative analysis of DSSCs fabricated via TiO_2 nanowire photoanodes and their performance.

Photoanode Type	**Synthesis Method**	**Dye**	**Electrolyte**	**PCE**	**Ref.**
DSSC with TiO_2 nanowire arrays	Vertically aligned single-crystalline TiO_2 nanowire arrays by nonpolar solvent/hydrophilic solid substrate interfacial reaction under hydrothermal conditions	N719	MPN-100 (Solaronix, Inc., Switzerland) containing tri-iodide in methoxy-propionitrile	5.02%	[56]
DSSC with TiO_2 nanowires and TiO_2 NPs	Double layered photoanode having corn like TiO_2 nanowires prepared by a surface tension stress mechanism	N719	Dimethylpropylimidazolium iodide, LiI, I_2, and 4-*tert*-butylpyridine in acetonitrile	7.11%	[58]
DSSC with thornbush like TiO_2 nanowires (TBWs)	Thornbush like TiO_2 nanowires (TBWs) prepared by a facile single step hydrothermal method	N719	Dimethylpropylimidazolium iodide, LiI, I_2, and 4-*tert*-butylpyridine in acetonitrile	6.7%	[63]
DSSC with TiO_2 nanowires and TiO_2 NPs	Double sided brush shaped (DSBS) TiO_2 nano architecture consisting of highly ordered TiO_2 nanowires aligned around an annealed TiO_2 nanoparticle	N719	1-Butyl-3-methyl imidazolium iodide, I_2, guanidinium thiocyanate, and 4-*tert*-butylpyridine in a mixture of acetonitrile and valeronitrile	5.61%	[59]

	layer was prepared by a hydrothermal method				
DSSC with TiO_2 nanowire	Vertically aligned anatase TiO_2 nanowires on FTO glass with a tunable length in the range of 15–55 mm for multilayered configuration of the photoanode by a hydrothermal method	N719	I^-/I_3^- redox electrolyte	9.40%	[60]
DSSC with multistacked three dimensional, hyperbranched titania nanoarchitectures	Photoelectrode with multistacked layers having integrated functions	N719	1-Methyl-3-propylimidazolium iodide (PMII), LiI guanidinium thiocyanate, I_2, and *tert*-butylpyridine in acetonitrile and valeronitrile	11.01%	[62]
DSSC with TiO_2 nanowires	Vertically aligned rutile TiO_2 nanowire arrays (NWAs) by a single step solvothermal method without using any surfactant or template	C106	DMII, LiI, I_2, TBP, and GNCS in the mixture of acetonitrile and valeronitrile	8.9%	[64]
DSSC with a TNW-AuNP hybrid structure	3D TNW-AuNP plasmonic electrode prepared by hydrothermal and sputtering techniques	N719	I_2, LiI, DMPII, and TBP in acetonitrile	9.73%	[61]
DSSC with a rutile TiO_2 nanowire array	Rough surface rutile TiO_2 nanowire array prepared by a hydrothermal method and prolonged etching. An additional light scattering layer of TiO_2 particles was also employed	C109	1,3-Dimethylimidazolium, lithium iodide, iodine, *tert*-butylpyridine, and guanidinium thiocyanate in acetonitrile and valeronitrile	9.39%	[65]

4.2. 1-D Nanorods

In order to improve the efficiency of DSSCs through the use of their special 1-D nanoscale properties, nanorods (NRs) have been introduced into the fabrication process of DSSCs. Due to their unique geometry, these TNRs have benefits in enhancing effective electron transport. The DSSCs can perform better overall by

integrating TNRs because they can lessen the ohmic loss that ordinarily happens during the electron transfer process through the mesoporous titania layer. Researchers have looked into numerous processes for creating TNRs exclusively for DSSC applications in order to acquire the needed characteristics. Additionally, as illustrated in **Figure 13**, they have worked very hard to change the morphology and surface characteristics of these nanorods.[55] These efforts include the development of novel synthesis techniques that allow TNRs to be customised to match the unique needs of DSSCs and further increase their efficacy.

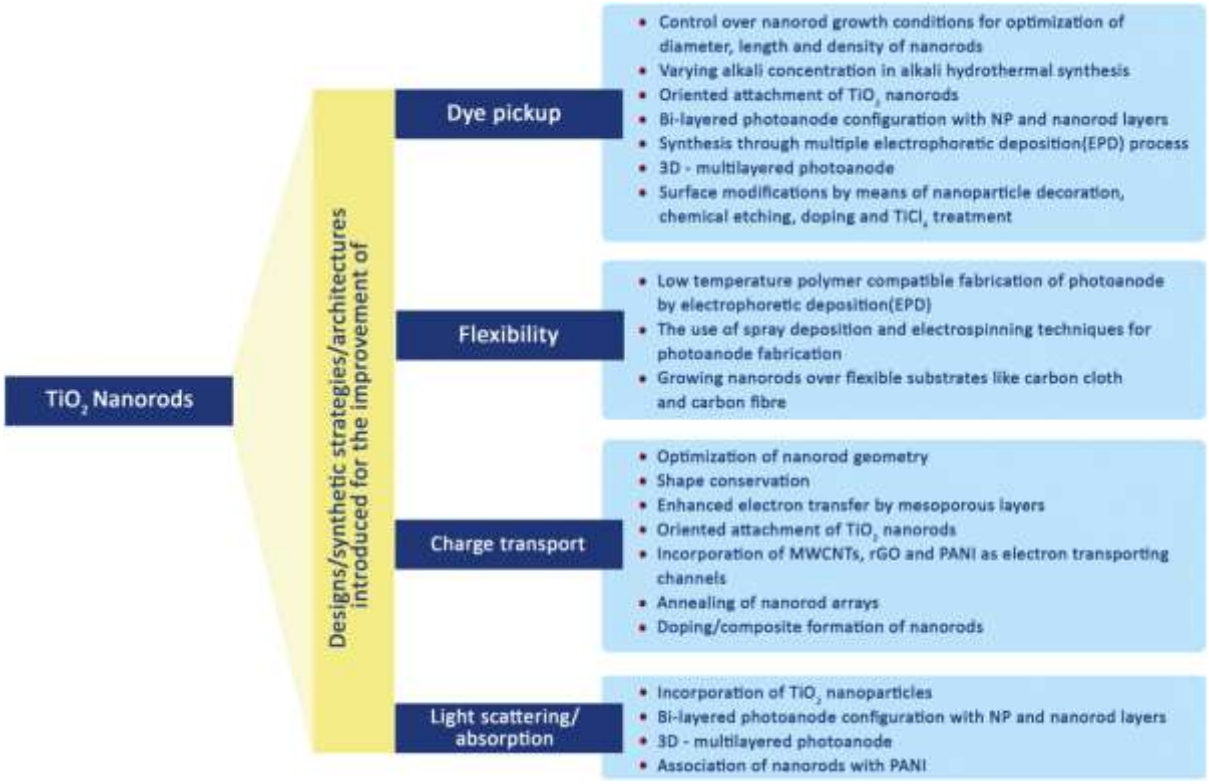

Figure 13. Various modifications made in TiO_2 nanorods to improve the DSSCs performance.[55]

In order to exert control over the size and diameter of the nanorods, Jiu *et al.* in 2006 successfully synthesised single-crystalline anatase TNRs using a surfactant-assisted hydrothermal method. The resultant nanorods had a length that ranged from 100 to 300 nm and a diameter of 20 to 30 nm. The incorporation of these TNRs into DSSCs allowed the researchers to obtain a noteworthy efficiency of 7.29%.[66] Because it permitted for improved electron transport qualities and more effective light absorption, the ability to adjust the size and diameter of the nanorods played a vital part in their efficacy within the DSSCs and eventually contributed to the better overall efficiency of the DSSC. This work by Jiu *et al.* opened up new opportunities for further developing solar cell technology by demonstrating the potential of using TNRs in DSSC photoanodes. De Marco *et al.* achieved a PCE of 7.9%, which represents a significant improvement in the performance of DSSCs. The utilisation of TNRs, which were made utilising a single-step solvothermal

method, allowed for this substantial improvement. The produced anatase TNRs were afterwards turned into a screen printable paste, making it simple to apply to DSSCs.[67]

Zhang *et al.* in their work suggested a unique method for fabricating anatase TNRs with controllable dimensions and shapes. They were able to create long, single-crystalline TNRs with reduced grain boundaries that improved charge collecting by using an orientated attachment technique. These long, skinny NRs allowed DSSCs to operate at an amazing 8.87% efficiency.[68] Parallelly, Liu *et al.* created a solvothermal technique to create single-crystalline anatase TNRs using tetrabutylammonium hydroxide (TBAH) as a morphology-controlling agent. The DSSCs created with the help of these nanorods had a noteworthy PCE of 8.66% (**Figure 14(a-b)**).[69] A notable development in DSSCs was made in 2009 by Lee *et al.*, who attained a remarkable efficiency of 9.52% as shown in **Figure 14(c-d)**. They used a hybrid of electrospinning and sol-gel methods to create TNRs from a solution of polyvinyl acetate and titanium *n*-propoxide in dimethyl formamide. They compared the performance of DSSCs based on nanoparticles and nanorods. Through their research, they noticed that the pore volume of the TNR-DSSCs was double that of the nanoparticle-DSSCs. When compared to nanoparticle-based DSSCs with comparable masses of TiO_2, the TNR-based DSSCs had almost 2.5 times as much surface area accessible as sensitizers.[70] Additionally, nanorods showed an 8-times prolonged electron-hole recombination time than nanoparticle DSSCs, indicating greater charge separation and retention. Multi-walled carbon nanotubes (MWCNTs) were incorporated into TNRs using the electrospinning method in 2013, which Yang *et al.* dubbed "electron transporting superhighways". The inventive addition of MWCNTs improved the DSSCs' efficiency even more, increasing it to an astonishing 10.24%.[71]

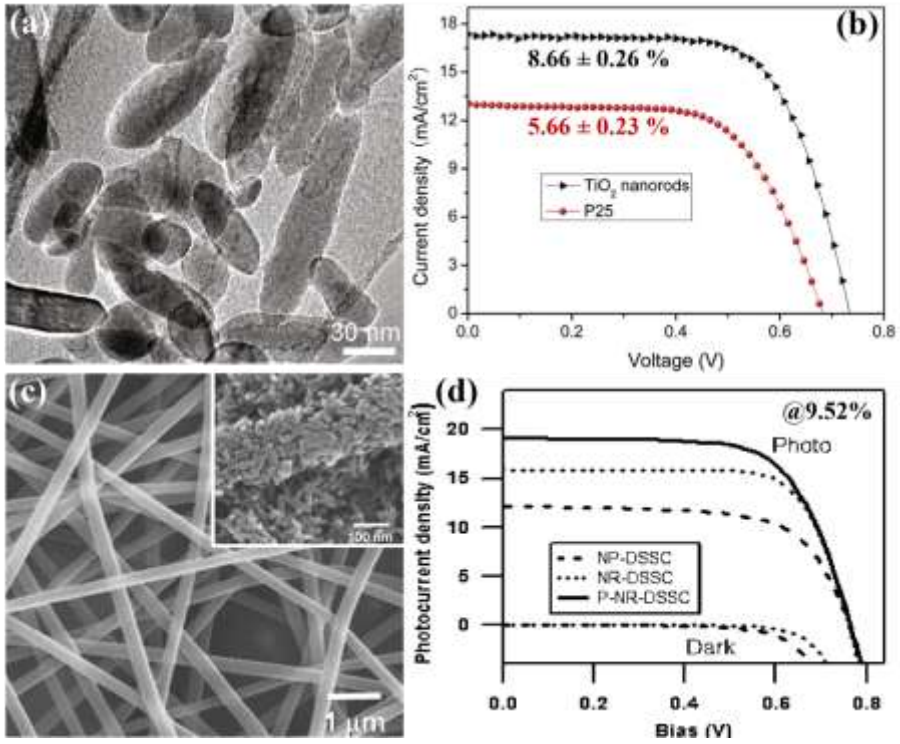

Figure 14. (*a-b*) High resolution TEM image of single crystalline anatase TiO_2 nanorods and the respective DSSC performance with 8.66% PCE,[69] (*c-d*) typical SEM image of electro-spun TiO_2-PVAs nanofibers with heat treated @400°C SEM image in inset and their consequent performance with PCE of 9.52%.[70]

There was subsequently a rise in interest in fusing other nanomaterials with TiO_2 nano-morphologies. One such notable photoanode material has a double-layered structure with ZnO nanoflowers embedded in TiO_2 as the bottom layer and TNRs as the top layer. Chen *et al.* invented this ground-breaking concept, and they did it by successfully achieving a PCE of 8.01%. This innovation demonstrates the investigation of innovative nanomaterial combinations to improve photoanode performance for possible use in photovoltaic devices.[72] Subramaniam *et al.* were succeeding in overlaying the TNR surface with a layer of reduced graphene oxide (rGO) in an effort to increase the charge collection efficiency of the nanorods. An outstanding PCE of 4.54% was achieved because to the addition of a 2 wt% rGO loaded nanocomposite, which greatly increased photoconversion efficiency.[73] Later studies by Tang and team revealed a connection between the efficacy and ability of dye loading on TNRs and their aspect ratios. They discovered that the dye loading efficiency and capacity both rose when the NRs' aspect ratios did. They managed the response time during the preparation procedure to produce nanorods with various aspect ratios.[74] Significant results from numerous investigations on TNR-based DSSCs are compiled in **Table 2**.

Table 2. Comparative analysis of DSSCs fabricated via TiO_2 nanorod photoanodes and their performance.

Photoanode Type	**Synthesis Method**	**Dye**	**Electrolyte**	**PCE**	**Ref.**
DSSC with TiO_2 nanorods	TiO_2 single crystalline anatase nanorods prepared by a surfactant assisted hydrothermal method	N719	LiI, 1,2-dimethyl-3-*n*-propylimidazolium iodide (DMPII), I_2, and 4-*tert*-butylpyridine (TBP) in methoxyacetonitride	7.06%	[75]
DSSC with TiO_2 nanorods	Highly crystalline TiO_2 nanorods synthesized by a hydrothermal process in a cetyltrimethylammonium bromide surfactant solution	N719	LiI, 1,2-dimethyl-3-*n*-propylimidazolium iodide (DMPII), I_2, and 4-*tert*-butylpyridine (TBP) in methoxyacetonitride	7.29%	[66]
DSSC with TiO_2 nanorods	TiO_2 nanorod based photoelectrodes prepared by a combination of sol–gel chemistry and electrospinning	N719	1-Butyl-3-methylimidazolium iodide, iodine, guanidinium thiocyanate, and 4-*tert*-butylpyridine in acetonitrile/valeronitrile	9.52%	[70]
DSSC with TiO_2 nanorods	TiO_2 anatase nanorods prepared by a simple one-step solvothermal method	N719	LiI, I_2, 1-methyl-3-propylimidazolium iodide, and *tert*-butylpyridine in dried acetonitrile	7.9%	[67]
DSSC with TiO_2 NRs/NPs	1 : 1 TiO_2 NR-NP composites prepared by a hydrothermal technique with a hydrogen titanate nanorod precursor	N719	LiI, I_2 and 4-*t*-butylpyridine in acetonitrile	8.61%	[76]
DSSC with TiO_2 nanorods having a composite structure	Ultraporous anatase TiO_2 nanorods fabricated by a simple microemulsion electrospinning approach	N719	I_2, LiI, 1-methyl-3-propylimidazolium iodide (PMII), guanidinium	8.53%	[77]

			thiocyanate, and *tert* butylpyridine in a mixture of acetonitrile/valeronitrile		
DSSC with a spherical TiO_2 nanorod-aggregate light-scattering layer	TiO_2 microspheres assembled by single crystalline rutile TiO_2 nanorods were synthesized by one-pot solvothermal treatment	N719	I_2, LiI, 1-methyl-3-propylimidazolium iodide (PMII), guanidinium thiocyanate, and *tert*-butylpyridine in a mixture of acetonitrile/valeronitrile	8.22%	[78]
DSSC with TiO_2 nanorods and MWCNTs	MWCNTs are introduced into TiO_2 nanorods by electrospinning	N719	I_2, LiI, 1-methyl-3-propylimidazolium iodide (PMII) and 4-*tert*-butylpyridine in a mixture of acetonitrile/valeronitrile	10.24%	[71]
DSSC with TiO_2 nanorods	Single crystal-like anatase TiO_2 nanorods with a specific growth direction are prepared by a hydrothermal method	Z907	1,3-Dimethylimidazolium iodide, LiI, and I_2 in a mixture of acetonitrile and valeronitrile	8.87%	[68]
DSSC with TiO_2 nanorods	Single-crystalline anatase TiO_2 nanorods were prepared by a solvothermal method	N719	LiI, I_2, dimethylpropylimidazolium iodide (DMPImI) and *tert*-butylpyridine in dry acetonitrile	8.66%	[69]
DSSC with TiO_2 nanorods	Monodispersed TiO_2 nanorods were prepared using a simple solvothermal process	N719	Lithium iodide, iodine, 4-*tert*-butylpyridine and 1,2-dimethyl-3-propylimidazolium iodide was dissolved in acetonitrile	9.21%	[79]
DSSC with TiO_2 nanorods	Single-crystalline anatase TiO_2 nanorods with a high aspect ratio	N719	LiI, I_2, dimethylpropylimidazolium iodide (DMPImI)	7.51%	[74]

			and *tert*-butylpyridine in a dry mixed solution		
DSSC with TiO_2/ZnO nanoflowers and TiO_2 nanorod array	Double layered photoanode having an overlayer of a TiO_2 NR array and underlayer of a TiO_2 embedded ZnO nanoflower array by a sol–gel method	N719	LiI, I_2 and $LiClO_4$ in acetonitrile	8.01%	[72]
DSSC with rutile TiO_2 nanorods incorporated with α alumina	Rutile TiO_2 nanorods incorporated with α alumina were developed on an FTO surface *via* a hydrothermal route	N719	KI, I_2 and 4-*tert*-butyl pyridine	6.5%	[80]

4.3. 1-D nanotubes

TiO_2 nanotubes (TNTs), which have a distinctive hollow cavity architecture and a much greater active surface area, were the subject of research. TNTs generally showing exceptional abilities in terms of increased absorption capacity and quick electron transport, making them particularly appropriate for use in DSSCs. TiO_2 meso-structures can successfully avoid the emergence of electron traps by using nanotube arrays with small spaces between them. The diffusion length, which measures the distance an electron may travel inside a tube before engaging in recombination, is significantly improved as a result of this estimated strategy. According to calculations, a nanotube cell's diffusion length is approximately 100 μm.[81] In order to increase the surface area while also lowering the likelihood of recombination, the size of the nanotubes can be extended up to this threshold. TNTs have some disadvantages, chief among them the high cost of production and time-consuming preparatory procedures needed. The morphology and crystalline structure of the TNTs used in DSSCs have a significant impact on their efficiency. Contrary to popular belief, it has been found that decreasing tube diameter has a greater positive influence on efficiency improvement than increasing tube length. The annealing temperature that the nanotubes go through also affects how much dye is put onto them. Harvesting efficiency is another important aspect that affects performance, and it can be improved by making changes to the tube surfaces that reduce recombination losses.[82] The efforts made to improve the efficiency of TNT-based DSSCs are shown in **Figure 15**.[55]

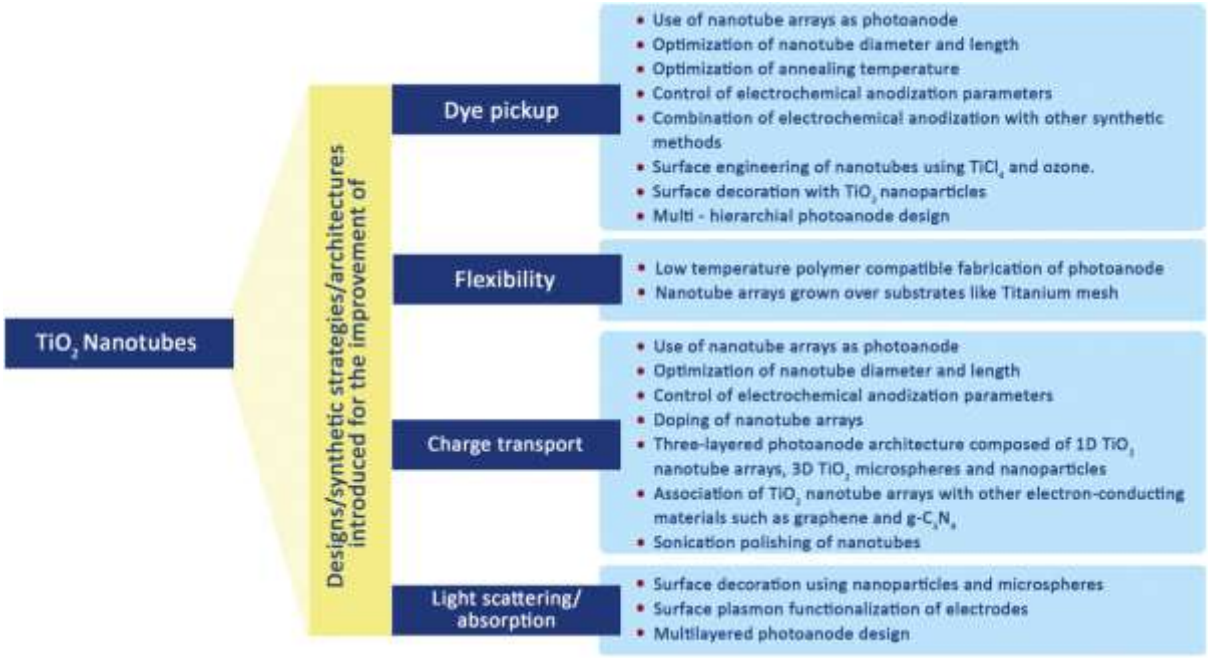

Figure 15. Various modifications made in TiO_2 nanotubes to improve the DSSCs performance.[55]

A study by Wang *et al.* showed that TNT-arrays in DSSCs can be made more effective by being treated with $TiCl_4$ and ozone. They attained an efficiency of 7.37% by using this surface engineering strategy and shown in **Figure 16(a-b)**.[83] Similar to this, Lei *et al.* used 1-D TNT-arrays made by anodization to reach an efficiency of 8.07% (**Figure 16(c-d)**).[84] Another study by Hun Park *et al.* revealed that after undergoing a treatment with $TiCl_4$, TNTs longer than 15 μm that were transplanted onto an FTO plate had an PCE of 5.36%.[85] Researchers looked into adding dopants to TNT-arrays alongside to surface engineering to increase performance. They intended to obtain an ideal alignment between the LUMO of dye molecules and the conduction band of TNTs in order to facilitate effective electron transfer. It was predicted that this alignment would improve electron injection and decrease electron recombination, improving overall efficiency. Numerous research teams investigated other strategies to doping to improve TNT-arrays in DSSCs, such as surface decorating with nanoparticles and microspheres. It was shown by Roy *et al.* that treating TNTs with $TiCl_4$ caused the TNT surface to be decorated with TiO_2 nanocrystals. The overall efficiency was raised as a result of the much-increased dye absorption provided by the surface ornamentation.[86] He *et al.* used a different strategy by using microwave created TiO_2 microspheres to decorate a TiO_2 NTA. This method has the potential to improve the functionality of DSSCs because the addition of these microspheres led to an efficiency of 7.24%.[87]

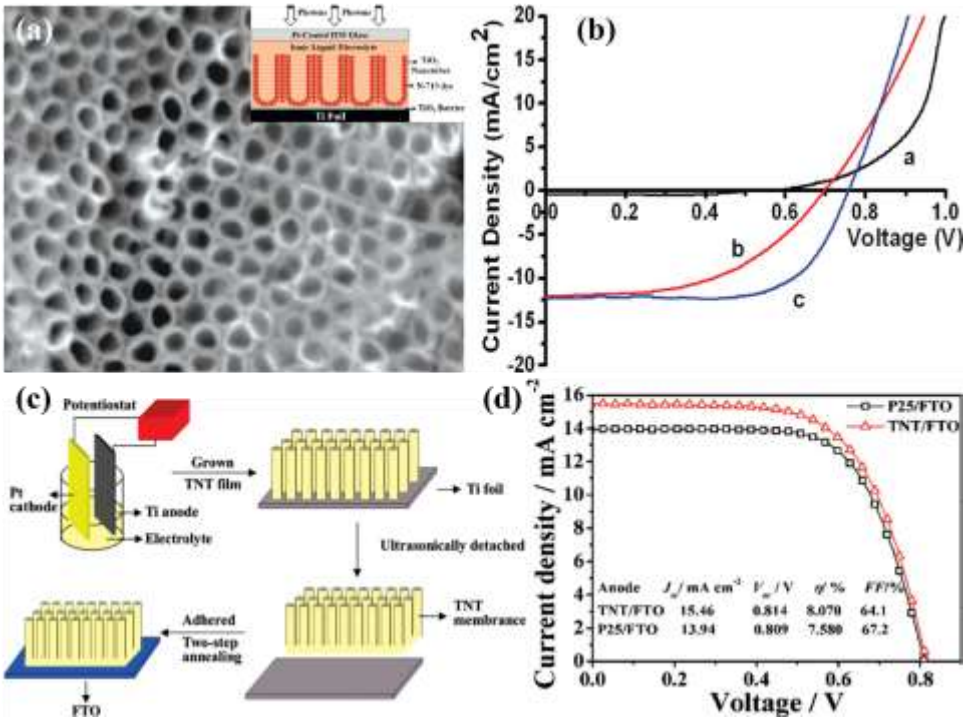

Figure 16. (*a*) FESEM top-view of highly ordered TiO_2 nanorod arrays and inset image is a schematic illustration of fabricated DSSC, (*b*) *J-V* characteristics of the prepared device (black: under dark light, red: without $TiCl_4$ treated anatase TiO_2 nanotube array, and blue: $TiCl_4$ treated TiO_2 based DSSC),[83] (*c*) schematic procedure of fabricating crystallized TiO_2 nanotubes on FTO substrate, (*d*) Comparative *J-V* analysis using the same thickness (20.8 μm) of TiO_2 nanotubes/FTO film and P25/FTO film under AM 1.5G illumination (100 mW cm^{-2}).[84]

By creating an intriguing multi-hierarchical photoanode with a cigar-shaped Au/TiO_2 nanotube array/TiO_2 nanoparticle structure in 2019, Fu *et al.* accomplished a substantial development. This photoanode had an amazing PCE of 8.93% (**Figure 17(a-b)**).[88] A novel vacuum-assisted colloid filling method was used to develop this one-of-a-kind multi-hierarchical design, which led to a photoanode with four times better charge transfer and 3.2 times greater dye intake than standard TNT array-based photoanodes. A hybrid photoanode that combines ZnO nanorods with TNTs was proposed by Cirak *et al.* in a different work.[89] This hybrid photoanode was created using a two-step synthetic procedure that started with the anodic oxidation of TNTs and ended with the hydrothermal layering of ZnO nanorods on top of the TNTs. This hybrid strategy shows promise in improving photoanode effectiveness for prospective use in DSSC. Comparing the hybrid design to the conventional TNT photoanode, the PCE was increased by around a factor of two.

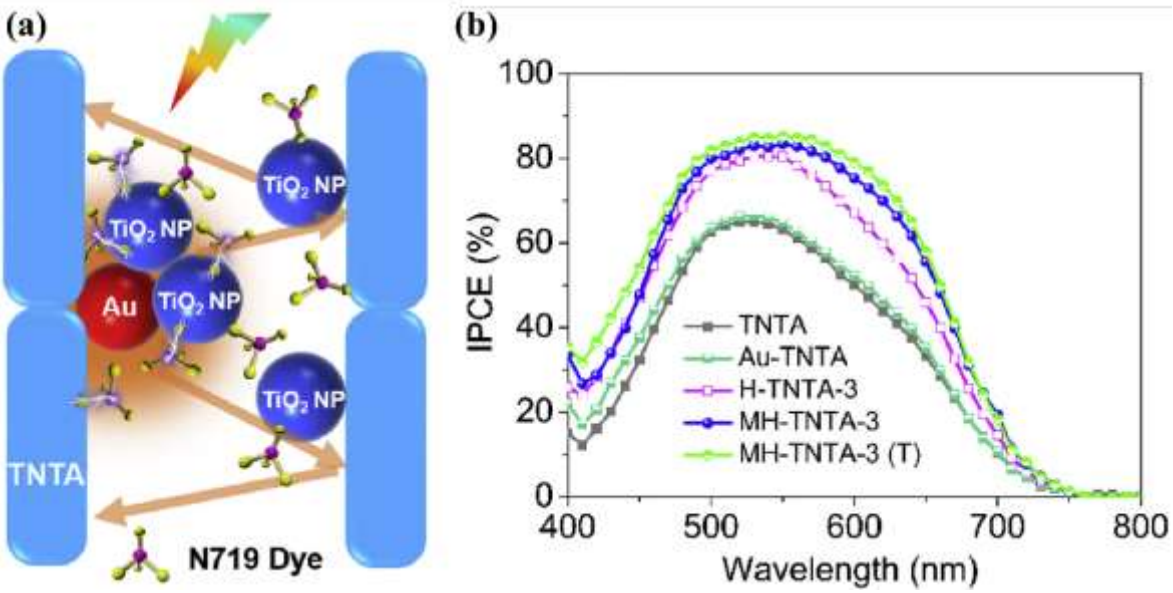

Figure 17. (*a*) Schematic illustration of Au-NPs induced plasmonic effect and enhanced light-trapping effect in the MH-TNTA film, (*b*) Consequent IPCE spectra of DSSCs based on various photoanodes.[88]

A ground-breaking 3-layered photoanode structure of 1D TNT-arrays, 3D TiO_2 microspheres, and 0-D nanoparticles was developed by Wu *et al.* in 2014. This creative design displayed outstanding inherent characteristics, such as a high dye loading capacity, effective light scattering performance, and improved charge collection ability. These beneficial characteristics allowed this innovative structure to achieve an unparalleled 9.10% PCE.[90] In order to further investigate and improve their performance, multiple other research groups have imitated this technique by producing tri-layered photoanodes with a variety of changes. In general, many techniques for altering TNTs have been employed, which includes (a) gluing on light-harvesting molecules for sensitization of nanotubes, (b) doping with multiple components, (c) band gap tuning, (d) developing electronic heterojunctions, and (e) furnishing with additional semiconductor particles.[91] An overview of the many uses of tubular TiO_2 nanoparticles in DSSCs is given in **Table 3.**

Table 3. Comparative analysis of DSSCs fabricated via TiO_2 nanotubes photoanodes and their performance.

Photoanode Type	Synthesis Method	Dye	Electrolyte	PCE	Ref.
DSSC with TiO_2 nanotubes	Titania nanotubes were synthesized using molecular assemblies	N3	0.03 M iodine in 0.3 M lithium iodide in 3-methyl-2-oxazolidinone (NMO)/acetonitrile	4.88%	[92]
DSSC with a TiO_2 nanotube array	Highly ordered TiO_2 nanotube arrays were fabricated by electrochemical anodization followed by surface engineering using $TiCl_4$ and O_2 plasma	N719	BMIM-I, I_2, TBP, and GTC in acetonitrile/valeronitrile	7.37%	[83]
DSSC with a TiO_2 nanotube array	Highly ordered one-dimensional TiO_2 nanotube arrays were prepared by anodization of pieces of Ti foil	N719	I_2, 1-methyl-3-propylimidazolium iodide (PMII), guanidinium thiocyanate, and *tert*-butylpyridine in acetonitrile and valeronitrile	8.07%	[84]
DSSC with a TiO_2 nanotube array/NPs	Layer-by-layer assembly of self-standing titania nanotube arrays and NPs were prepared by anodization	Ru535-bisTBA	1,2-dimethyl-3-propyl imidazolium iodide, LiI, I_2, and 4-*tert*-butylpyridine in acetonitrile	8.80%	[93]
DSSC with TiO_2 nanotubes and TiO_2 microspheres	TNTAs were prepared by anodization of pieces of Ti foil in an aqueous solution containing hydrofluoric acid and TiO_2 scattering microspheres were prepared *via* a microwave solvothermal process	N719	I_2, 1-methyl-3-propylimidazolium iodide (PMII), guanidinium thiocyanate, and *tert*-butylpyridine in a solution of valeronitrile and acetonitrile	7.24%	[87]
DSSC with TiO_2 nanotube/microsphere/NPs tri-layered photoanode	Double layered photoanode with a 1D NT underlayer and 3D hierarchical upper layer was prepared by a hydrothermal method and then incorporated with hydrothermally prepared TiO_2 NPs	N719	1-Methyl-3-propylimidazolium iodide (PMII), guanidinium thiocyanate, I_2, LiI, and *tert*-butylpyridine dissolved in acetonitrile and valeronitrile	9.10%	[90]
DSSC with a composite of P25 NP/TiO_2 NTA/flower like TiO_2	TiO_2 NTAs prepared by anodization were transplanted on to a P25 coated FTO plate and then flower like	N719	LiI, I_2, 4-*tert*-butylpyridine and 1, 2-dimethyl-3-propylimidazolium iodide (DMPII) in dry acetonitrile	6.48%	[94]

	TiO_2 prepared hydrothermally was deposited over a P25/NTA film				
DSSC with a Au/TiO_2 nanotube array/TiO_2 nanoparticle photoanode	"Cigar-like" Au/TiO_2-nanotube-array/TiO_2-nanoparticle multi-hierarchical photoanode through a novel vacuum-assisted colloid-filling approach	N719	LiI, I_2, 1-methyl-3-hexylimidazolium iodide (HMII), *N*-methylbenzimidazole (NMB) and 4-*tert*-butylpyridine in 3-ethoxypropionitrile	8.93%	[88]
DSSC with a tri-layered photoanode	Tri-layered photoanode consisting of single crystal hollow TiO_2 nanoparticles (HTNPs), sub-micro hollow TiO_2 mesospheres (SHTMSs) and hierarchical TiO_2 microspheres (HTMSs)	N719	1-Methyl-3-propylimidazo-lium iodide (PMII), guanidinium thiocyanate, I_2, LiI, and *tert*-butylpyridine dissolved in acetonitrile and valeronitrile	9.24%	[95]
DSSC with an open ended TiO_2 nanotube array photoanode	Open ended TiO_2 nanotube array photoanode was prepared by fast removal of bottom caps by mechanical ball milling	N719	LiI, I_2, 1-methyl-3-hexylimidazolium iodide (HMII), *N*-methylbenzimidazole (NMB), and 4-*tert*-butylpyridine in 3-methoxypropionitrile	7.7%	[96]

5. Charge Transport and Electronic Analogy

1-D TiO_2 nanostructures have distinct advantages over bulk TiO_2 with a wide bandgap, including increased surface area, a large number of active sites, and the impact of quantum confinement phenomena. The size, unique crystal facets, shape, and synchronisation of these nanostructures, as well as their alignment, are the main determinants of their electrical characteristics. Quantum confinement factors cause the bandgap to widen when nanowire size approaches the nanoscale regime. Doping with foreign elements is the main tactic used to adjust the bandgap and realign the valence and conduction band configurations favourably with the sensitizer energy levels. With the use of this method, one can tune their electrical characteristics precisely,

improving their functionality for uses in DSSC. Vertically arranged nanowire-based photoanodes have been used to provide the most outstanding DSSC performances. In nanorods, a large decrease in the grain boundaries, which frequently serve as electron traps, results in a boost in the electron diffusion length and, as a result, better charge transfer. TNRs aspect ratio can be changed in order to change the bandgap. The conduction band edge shifts downward as the aspect ratio of nanorods rises. Similar to this, adding surface roughness and meso-porosity can increase the surface area of nanorods, further boosting their performance in DSSCs. These techniques are essential for enhancing the electrical characteristics and effectiveness of photoanodes based on nanorods for cutting-edge solar cell applications. Quantum confinement effects, an exciting phenomenon only seen in hydrothermal tubes, are shown in TNTs with a wall thickness below 5 nm. The abundance of oxygen vacancies and Ti^{3+} ions is another element enhancing charge transmission in these nanotubes. The potential of these nanotubes to transfer charges is significantly influenced by the annealing temperature. Numerous techniques, such as doping, surface adsorption, the creation of heterojunctions, and surface embellishment, can be used to design the bandgap in nanotubes. With the help of these techniques, the bandgap of the nanotubes may be precisely altered, affecting its electrical characteristics and, as a result, improving their efficiency in future applications, such as DSSC.[70][97][98][99][100][101]

6. Importance of 1-D TiO_2 Nanorods

Notably in the area of photovoltaics industry, 1-D TiO_2 photoanodes are essential for energy conversion. They are important for a number of reasons:

Increased light absorption: Unlike to conventional TiO_2 thin films, 1-D TiO_2 nanostructures, such as nanowires, nanotubes, nanobelts or nanoneedles, offer an enormously huge surface area-to-volume ratio. This feature makes it feasible to use sunlight more effectively, improving the device's overall ability to convert photo energy into electrical energy.[102][103][104]

Superior charge transport: For photogenerated electrons and holes, 1-D TiO_2 structures offer effective charge transport channels. Longer carrier lifetimes and larger photocurrents are produced as a consequence of the dearth of defects and grain boundaries in these structures. Higher energy conversion efficiencies are a result of this enhanced charge transport.[105][106][107]

Tunability of the bandgap: The 1-D structures' size and shape can be changed by doping etc. to alter the bandgap of TiO_2. The bandgap can be tuned for better alignment with the solar spectrum and more effective solar energy harvesting.[108][109]

Stability and Durability: 1-D TiO_2 structures display outstanding chemical stability and photo-corrosion resistance. This characteristic makes the photoanodes excellent for long-term energy conversion applications since it guarantees that they can endure repeated exposure to adverse weather conditions.[110][111][112]

Flexibility: 1-D TiO_2 structures are readily incorporated into a wide range of device topologies, including DSSCs, perovskite solar cells, and quantum dot solar cells. They are adaptable components in energy conversion systems because of their compatibility with various materials and fabrication processes.[11][113]

Moreover, other than application in photovoltaics, 1-D TiO_2 nanostructures like nanotubes, nanowires, nanobelts, and nanorods, have been regarded as highly desirable candidates for a number of uses, including the photocatalytic degradation of pollutants, the photocatalytic conversion of CO_2 into energy fuels, water splitting, supercapacitors, and lithium-ion batteries. Therefore, the remarkable properties of 1-D TiO_2 nanostructures, ranging from enhanced light absorption and charge transport to tunability of bandgap and exceptional stability, position them as versatile and vital components not only in photovoltaics but also in a wide array of sustainable energy and environmental applications, showcasing their potential to drive advancements in renewable energy and catalysis technologies.

7. Future Perspective

Future evolutions in 1-D TiO_2 nanostructures have enormous potential to influence the development of sustainable and energy-conversion technologies. Even more significant advancements in this area are probably possible with continued research and invention. These nanostructures might be crucial in solving crucial energy challenges:

Enhanced Efficiency: We anticipate being able to precisely build 1-D TiO_2 structures with respect to their attributes as our knowledge of nanoscale processes expands. This might lead to even better energy conversion efficiency, overcoming present constraints and boosting the affordability of renewable energy sources.

Multifunctionality: New functions of 1-D TiO_2 structures may be discovered in the future study, allowing them to work as both energy conversion platforms and sensors, enhancing their effect in fields like smart energy grids and real-time environmental monitoring.

Integration and Hybridization: Joint initiatives to combine 1-D TiO_2 nanostructures with other cutting-edge substances, such as perovskites or quantum dots, may produce synergistic effects that maximize energy capture, transfer, and storage, resulting in more effective and flexible systems.

Beyond photovoltaics: 1-D TiO_2 nanostructures' adaptability could expand the range of industries in which they are used, such as thermoelectric, where their special features could be used to convert waste heat into electricity and so improve energy efficiency.

Energy Storage Revolution: The incorporation of 1-D TiO_2 structures into energy storage systems, such as lithium-ion batteries and supercapacitors, could usher in a new era of energy storage technologies that offer quicker charging times, longer lifespans, and greater safety.

CO_2 Utilisation and Catalysis: In the context of sustainable chemistry, 1-D TiO_2 nanostructures could catalyse the conversion of CO_2 into useful fuels or chemicals, assisting in the shift to a society that emits no carbon.

Large-Scale Manufacturing: For 1-D TiO_2 nanostructures to be widely used, it will be essential to scale up production. Making these technologies economically feasible will depend heavily on the development of scalable, cost-effective production processes.

Global Sustainability: The use of 1-D TiO_2 nanostructures in underdeveloped countries may offer clean energy options where conventional infrastructure is weak, assisting with efforts to promote global sustainability and ensure that everyone has access to energy.

Fundamentally, 1-D TiO_2 nanostructures have a bright future in energy conversion and sustainable technology. These structures have the potential to alter our energy environment and usher in a more sustainable and resilient future as interdisciplinary collaborations bloom and as our understanding of nanomaterials advances.

8. Conclusion

This review delves a thorough overview of 1-D TiO_2-based photoanode materials used in DSSCs, and it digs into the intricate designs and operating principles of various TiO_2 nanostructures. The globe is heavily dependent on non-renewable energy sources, which has resulted in significant environmental damage and resource depletion. This leads to interest in solar energy's conversion to both electricity and hydrogen fuel as it emerges as an abundant and absolutely free energy source. A potential solution to the coming energy issue is solar cells, which act as agents that convert sunlight into electrical power. Notably, numerous TiO_2 nanostructures have recently been created for use as photoanodes in DSSCs, including nanoparticles, nanowires, nanorods, and nanotubes. These one-dimensional nanostructures are very promising candidates for creating effective DSSC photoanodes attributed to their exceptional light-scattering characteristics and quick electron transport. They can potentially achieve even better efficiency by surmounting their surface area-related stipulations. TiO_2 is more desirable than other semiconductors because of how well its band structure aligns with that of the sensitizer and because of how well it facilitates charge transport as a result. Notably, this attractiveness is further enhanced by its non-toxic nature and strong functional architecture. According to recent research, increasing TiO_2's infrared (IR) absorption capabilities can be achieved by prolonging its absorption threshold into the IR region, providing greater opportunities for charge collection.

This thorough analysis highlights the importance of 1-D TiO_2-based photoanode materials for developing DSSCs, highlighting their potential to address energy challenges amid the world's reliance on non-renewable sources, while highlighting their role in achieving efficient energy conversion through intricate designs and alignment with renewable solar resources.

CRediT authorship contribution statement

Kumar Vaisno Srivastava: Conceptualization, Validation, Investigation, Methodology, Formal analysis, Writing – original draft. **Raj Kumar Maurya:** Formal Analysis and Supervision. **Yatendra Pal Singh:** Writing – original draft and Supervision.

Acknowledgement

KVS, YPS, and RKM acknowledges the Department of Physics, Mangalayatan University and Department of Physics, RML University Faizabad for providing laboratory support and guidance. KVS also

extending his acknowledgement to Abhishek Srivastava, Senior Research Fellow-IIT Indore for being integral part throughout this work. All authors are thankful to Prof. Ravikant, Dean-Research and Development, Mangalayatan University.

Data Availability Statement

All data used will be made available by the corresponding author on reasonable request.

Conflict of Interest

There is no conflict to declare.

References

[1] F. Pietro Colelli, J. Emmerling, G. Marangoni, M.N. Mistry, E. De Cian, Increased energy use for adaptation significantly impacts mitigation pathways, Nat. Commun. 13 (2022) 1–12. https://doi.org/10.1038/s41467-022-32471-1.

[2] L.-E. British Oil and Gas Company, BP, Statistical Review of World Energy, n.d. https://www.bp.com/en/global/corporate/energy-economics/statistical-review-of-world-energy.html.

[3] M. Green, E. Dunlop, J. Hohl-Ebinger, M. Yoshita, N. Kopidakis, X. Hao, Solar cell efficiency tables (version 57), Prog. Photovoltaics Res. Appl. 29 (2021) 3–15. https://doi.org/10.1002/pip.3371.

[4] M. Grätzel, Dye-sensitized solar cells, J. Photochem. Photobiol. C Photochem. Rev. 4 (2003) 145–153. https://doi.org/10.1016/S1389-5567(03)00026-1.

[5] M. Freitag, J. Teuscher, Y. Saygili, X. Zhang, F. Giordano, P. Liska, J. Hua, S.M. Zakeeruddin, J.E. Moser, M. Grätzel, A. Hagfeldt, Dye-sensitized solar cells for efficient power generation under ambient lighting, Nat. Photonics. 11 (2017) 372–378. https://doi.org/10.1038/nphoton.2017.60.

[6] Brian O'Regan & Michael Grätzel, A low-cost, high-efficiency solar cell based on dye-sensitized colloidal TiO_2 films, Nature. 354 (1991) 737–740.

[7] K. Kakiage, Y. Aoyama, T. Yano, K. Oya, J.I. Fujisawa, M. Hanaya, Highly-efficient dye-sensitized solar cells with collaborative sensitization by silyl-anchor and carboxy-anchor dyes, Chem. Commun. 51 (2015) 15894–15897. https://doi.org/10.1039/c5cc06759f.

[8] Z. Tang, J. Wu, M. Zheng, J. Huo, Z. Lan, A microporous platinum counter electrode used in dye-sensitized solar cells, Nano Energy. 2 (2013) 622–627. https://doi.org/10.1016/j.nanoen.2013.07.014.

[9] A.S.H. Luque, Handbook of photovoltaic science and engineering, 2011.

[10] V. Sugathan, E. John, K. Sudhakar, Recent improvements in dye sensitized solar cells: A review, Renew. Sustain. Energy Rev. 52 (2015) 54–64. https://doi.org/10.1016/j.rser.2015.07.076.

[11] K. Sharma, V. Sharma, S.S. Sharma, Dye-Sensitized Solar Cells: Fundamentals and Current Status, Nanoscale Res. Lett. 13 (2018). https://doi.org/10.1186/s11671-018-2760-6.

[12] S. Ilic, V. Paunovic, Characteristics of curcumin dye used as a sensitizer in dye-sensitized solar cells, Facta Univ. - Ser. Electron. Energ. 32 (2019) 91–104. https://doi.org/10.2298/fuee1901091i.

[13] R. Katoh, A. Furube, Electron injection efficiency in dye-sensitized solar cells, J. Photochem. Photobiol. C Photochem. Rev. 20 (2014) 1–16. https://doi.org/10.1016/j.jphotochemrev.2014.02.001.

[14] J.A. Anta, I. Mora-Seró, T. Dittrich, J. Bisquert, Dynamics of charge separation and trap-limited electron transport in TiO_2 nanostructures, J. Phys. Chem. C. 111 (2007) 13997–14000. https://doi.org/10.1021/jp0737909.

[15] J.-J.L. Narayan Chandra Deb Nath, Binary redox electrolytes used in dye-sensitized solar cells, J. Ind. Eng. 78 (n.d.) 53–65. https://doi.org/https://doi.org/10.1016/j.jiec.2019.05.018.

[16] A.J. Frank, N. Kopidakis, J. Van De Lagemaat, Electrons in nanostructured TiO_2 solar cells: Transport, recombination and photovoltaic properties, Coord. Chem. Rev. 248 (2004) 1165–1179. https://doi.org/10.1016/j.ccr.2004.03.015.

[17] M. Grätzel, Conversion of sunlight to electric power by nanocrystalline dye-sensitized solar cells, J. Photochem. Photobiol. A Chem. 164 (2004) 3–14. https://doi.org/10.1016/j.jphotochem.2004.02.023.

[18] M.A. Green, Solar cell fill factors: General graph and empirical expressions, Solid State Electron. 24 (1981) 788–789. https://doi.org/10.1016/0038-1101(81)90062-9.

[19] Y. Gao, G. Lei, Z. Tian, H. Zhu, L. Ma, Photoelectrochemical Water Splitting, 2022. https://doi.org/10.1002/9783527830084.ch7.

[20] G. Uddin, Development of Simplified In Situ Processing Routes for Rear-Side Patterning of Silicon Heterojunction Interdigitated Back Contact (SHJ-IBC) Solar Cells, (2018) 90. https://www.researchgate.net/figure/Schematic-of-XPS-measurement-technique-61_fig16_331023989%0Afile:///C:/Users/pc/Downloads/MScThesis_Gius_UEF.pdf.

[21] K. Zhu, N. Kopidakis, N.R. Neale, J. Van De Lagemaat, A.J. Frank, Influence of surface area on charge transport and recombination in dye-sensitized TiO_2 solar cells, J. Phys. Chem. B. 110 (2006) 25174–25180. https://doi.org/10.1021/jp065284.

[22] J.M.K.W. Kumari, N. Sanjeevadharshini, M.A.K.L. Dissanayake, G.K.R. Senadeera, C.A. Thotawatthage, The effect of TiO_2 photo anode film thickness on photovoltaic properties of dye-sensitized solar cells, Ceylon J. Sci. 45 (2016) 33. https://doi.org/10.4038/cjs.v45i1.7362.

[23] P. Wang, S.M. Zakeeruddin, R. Humphry-Baker, J.E. Moser, M. Grätzel, Molecular-Scale Interface Engineering of TiO_2 Nanocrystals: Improving the Efficiency and Stability of Dye-Sensitized Solar Cells, Adv. Mater. 15 (2003) 2101–2104. https://doi.org/10.1002/adma.200306084.

[24] F. De Angelis, S. Fantacci, A. Selloni, Alignment of the dye's molecular levels with the TiO_2 band edges in dye-sensitized solar cells: A DFT-TDDFT study, Nanotechnology. 19 (2008). https://doi.org/10.1088/0957-4484/19/42/424002.

[25] D. Chen, F. Huang, Y.B. Cheng, R.A. Caruso, Mesoporous anatase TiO_2 beads with high surface areas and controllable pore sizes: A superior candidate for high-performance dye-sensitized solar cells, Adv. Mater. 21 (2009) 2206–2210. https://doi.org/10.1002/adma.200802603.

[26] K. Zhu, N.R. Neale, A. Miedaner, A.J. Frank, Enhanced charge-collection efficiencies and light scattering in dye-sensitized solar cells using oriented TiO_2 nanotubes arrays, Nano Lett. 7 (2007) 69–74. https://doi.org/10.1021/nl062000o.

[27] P.J. Cameron, L.M. Peter, Characterization of Titanium Dioxide Blocking Layers in Dye-Sensitized Nanocrystalline Solar Cells, J. Phys. Chem. B. 107 (2003) 14394–14400. https://doi.org/10.1021/jp030790+.

[28] S. Pace, A. Resmini, I.G. Tredici, A. Soffientini, X. Li, S. Dunn, J. Briscoe, U. Anselmi-Tamburini,

Optimization of 3D ZnO brush-like nanorods for dye-sensitized solar cells, RSC Adv. 8 (2018) 9775–9782. https://doi.org/10.1039/c7ra13128c.

[29] M.G. Ju, M. Chen, Y. Zhou, H.F. Garces, J. Dai, L. Ma, N.P. Padture, X.C. Zeng, Earth-Abundant Nontoxic Titanium(IV)-based Vacancy-Ordered Double Perovskite Halides with Tunable 1.0 to 1.8 eV Bandgaps for Photovoltaic Applications, ACS Energy Lett. 3 (2018) 297–304. https://doi.org/10.1021/acsenergylett.7b01167.

[30] X. Yu, W. Zeng, Fabrication and gas-sensing performance of nanorod-assembled SnO_2 nanostructures, J. Mater. Sci. Mater. Electron. 27 (2016) 7448–7453. https://doi.org/10.1007/s10854-016-4721-0.

[31] N. Prabavathy, S. Shalini, R. Balasundaraprabhu, D. Velauthapillai, S. Prasanna, P. Walke, N. Muthukumarasamy, Effect of solvents in the extraction and stability of anthocyanin from the petals of Caesalpinia pulcherrima for natural dye sensitized solar cell applications, J. Mater. Sci. Mater. Electron. 28 (2017) 9882–9892. https://doi.org/10.1007/s10854-017-6743-7.

[32] L.S.& J.R.D. Sacha Corby, Reshma R. Rao, The kinetics of metal oxide photoanodes from charge generation to catalysis, Nat. Rev. Mater. 6 (2021) pages1136–1155. https://doi.org/https://doi.org/10.1038/s41578-021-00343-7.

[33] M.B. Tahir, M. Rafique, M.S. Rafique, N. Fatima, Z. Israr, Metal oxide- and metal sulfide-based nanomaterials as photocatalysts, Elsevier Inc., 2020. https://doi.org/10.1016/b978-0-12-821192-2.00006-1.

[34] C.P. Lee, C.T. Li, K.C. Ho, Use of organic materials in dye-sensitized solar cells, Mater. Today. 20 (2017) 267–283. https://doi.org/10.1016/j.mattod.2017.01.012.

[35] A.P. K. B. Bhojanaa, A. Soundarya Mary, K. S. Shalini Devi, N. Pavithra, Account of Structural, Theoretical, and Photovoltaic Properties of ABO_3 Oxide Perovskites Photoanode-Based Dye-Sensitized Solar Cells, Sol. RRL. 6 (2022) 2100792. https://doi.org/https://doi.org/10.1002/solr.202100792.

[36] N. Baig, I. Kammakakam, W. Falath, I. Kammakakam, Nanomaterials: A review of synthesis methods, properties, recent progress, and challenges, Mater. Adv. 2 (2021) 1821–1871.

https://doi.org/10.1039/d0ma00807a.

[37] F.W. Low, C.W. Lai, Recent developments of graphene-TiO_2 composite nanomaterials as efficient photoelectrodes in dye-sensitized solar cells: A review, Renew. Sustain. Energy Rev. 82 (2018) 103–125. https://doi.org/10.1016/j.rser.2017.09.024.

[38] H. Siddiqui, Modification of Physical and Chemical Properties of Titanium Dioxide (TiO_2) by Ion Implantation for Dye Sensitized Solar Cells, Intech. (2019). https://doi.org/10.5772/intechopen.83566.

[39] A. Zatirostami, A dramatic improvement in the efficiency of TiO_2-based DSSCs by simultaneous incorporation of Cu and Se into its lattice, Opt. Mater. (Amst). 117 (2021) 111110. https://doi.org/10.1016/j.optmat.2021.111110.

[40] T.M. Mukametkali, B.R. Ilyassov, A.K. Aimukhanov, T.M. Serikov, A.S. Baltabekov, L.S. Aldasheva, A.K. Zeinidenov, Effect of the TiO_2 electron transport layer thickness on charge transfer processes in perovskite solar cells, Phys. B Condens. Matter. 659 (2023) 414784. https://doi.org/10.1016/j.physb.2023.414784.

[41] W. Zhang, Y. Liu, D. Zhou, H. Wang, W. Liang, F. Yang, Fast diffusion of silver in TiO_2 nanotube arrays, Beilstein J. Nanotechnol. 7 (2016) 1129–1140. https://doi.org/10.3762/bjnano.7.105.

[42] S. Jin, E. Shin, J. Hong, TiO_2 nanowire networks prepared by titanium corrosion and their application to bendable dye-sensitized solar cells, Nanomaterials. 7 (2017). https://doi.org/10.3390/nano7100315.

[43] H.G. Yang, G. Liu, S.Z. Qiao, C.H. Sun, Y.G. Jin, S.C. Smith, J. Zou, H.M. Cheng, G.Q. Lu, Solvothermal synthesis and photoreactivity of anatase TiO_2 nanosheets with dominant {001} facets, J. Am. Chem. Soc. 131 (2009) 4078–4083. https://doi.org/10.1021/ja808790p.

[44] P. V. Shinde, S. Gagare, C.S. Rout, D.J. Late, TiO_2 nanoflowers based humidity sensor and cytotoxic activity, RSC Adv. 10 (2020) 29378–29384. https://doi.org/10.1039/d0ra05007e.

[45] J. Liu, Q. Zhang, L. Niu, B. Hu, X. Zhou, Fabrication of mesoporous TiO_2 submicro/nanospheres with high specific surface and application in dye-sensitized solar cells, J. Mater. Sci. Mater. Electron. 27 (2016) 9115–9123. https://doi.org/10.1007/s10854-016-4946-y.

[46] D.C. Hurum, A.G. Agrios, K.A. Gray, T. Rajh, M.C. Thurnauer, Explaining the enhanced

photocatalytic activity of Degussa P25 mixed-phase TiO_2 using EPR, J. Phys. Chem. B. 107 (2003) 4545–4549. https://doi.org/10.1021/jp0273934.

[47] M. Landmann, E. Rauls, W.G. Schmidt, The electronic structure and optical response of rutile, anatase and brookite TiO_2, J. Phys. Condens. Matter. 24 (2012). https://doi.org/10.1088/0953-8984/24/19/195503.

[48] R. Asahi, Y. Taga, W. Mannstadt, Electronic and optical properties of anatase, Phys. Rev. B - Condens. Matter Mater. Phys. 61 (2000) 7459–7465. https://doi.org/10.1103/PhysRevB.61.7459.

[49] T. Umebayashi, T. Yamaki, H. Itoh, K. Asai, Analysis of electronic structures of 3d transition metal-doped TiO_2 based on band calculations, J. Phys. Chem. Solids. 63 (2002) 1909–1920. https://doi.org/10.1016/S0022-3697(02)00177-4.

[50] A. Khlyustova, N. Sirotkin, T. Kusova, A. Kraev, V. Titov, A. Agafonov, Doped TiO_2: The effect of doping elements on photocatalytic activity, Mater. Adv. 1 (2020) 1193–1201. https://doi.org/10.1039/d0ma00171f.

[51] A.F. Da Silva, N.S. Dantas, E.F. Da Silva, I. Pepe, M.O. Torres, C. Persson, T. Lindgren, J.S. De Almeida, R. Ahuja, Electronic and optical properties of TiO_2, AIP Conf. Proc. 772 (2005) 177–178. https://doi.org/10.1063/1.1994051.

[52] W. Guo, Y. Shen, G. Boschloo, A. Hagfeldt, T. Ma, Influence of nitrogen dopants on N-doped TiO_2 electrodes and their applications in dye-sensitized solar cells, Electrochim. Acta. 56 (2011) 4611–4617. https://doi.org/10.1016/j.electacta.2011.02.091.

[53] Sumio Iijima, Helical microtubules of graphitic carbon, Nature. 354 (1991) 56–58. https://doi.org/https://doi.org/10.1038/354056a0.

[54] M. Law, L.E. Greene, J.C. Johnson, R. Saykally, P. Yang, Nanowire dye-sensitized solar cells, Nat. Mater. 4 (2005) 455–459. https://doi.org/10.1038/nmat1387.

[55] D. Joshy, S.B. Narendranath, Y.A. Ismail, P. Periyat, Recent progress in one dimensional TiO_2 nanomaterials as photoanodes in dye-sensitized solar cells, Nanoscale Adv. 73 (2022) 5202–5232. https://doi.org/10.1039/d2na00437b.

[56] X. Feng, K. Shankar, O.K. Varghese, M. Paulose, T.J. Latempa, C.A. Grimes, Vertically aligned single crystal TiO_2 nanowire arrays grown directly on transparent conducting oxide coated glass: Synthesis details and applications, Nano Lett. 8 (2008) 3781–3786. https://doi.org/10.1021/nl802096a.

[57] W. Liu, H. Lu, M. Zhang, M. Guo, Controllable preparation of TiO_2 nanowire arrays on titanium mesh for flexible dye-sensitized solar cells, Appl. Surf. Sci. 347 (2015) 214–223. https://doi.org/10.1016/j.apsusc.2015.04.090.

[58] A.M. Bakhshayesh, M.R. Mohammadi, H. Dadar, D.J. Fray, Improved efficiency of dye-sensitized solar cells aided by corn-like TiO_2 nanowires as the light scattering layer, Electrochim. Acta. 90 (2013) 302–308. https://doi.org/10.1016/j.electacta.2012.12.065.

[59] C. Zha, L. Shen, X. Zhang, Y. Wang, B.A. Korgel, A. Gupta, N. Bao, Double-sided brush-shaped TiO_2 nanostructure assemblies with highly ordered nanowires for dye-sensitized solar cells, ACS Appl. Mater. Interfaces. 6 (2014) 122–129. https://doi.org/10.1021/am404942n.

[60] W.Q. Wu, Y.F. Xu, C.Y. Su, D. Bin Kuang, Ultra-long anatase TiO_2 nanowire arrays with multi-layered configuration on FTO glass for high-efficiency dye-sensitized solar cells, Energy Environ. Sci. 7 (2014) 644–649. https://doi.org/10.1039/c3ee42167h.

[61] Y.C. Yen, P.H. Chen, J.Z. Chen, J.A. Chen, K.J. Lin, Plasmon-induced efficiency enhancement on dye-sensitized solar cell by a 3D TNW-AuNP layer, ACS Appl. Mater. Interfaces. 7 (2015) 1892–1898. https://doi.org/10.1021/am507668j.

[62] W.Q. Wu, Y.F. Xu, H.S. Rao, C.Y. Su, D. Bin Kuang, Multistack integration of three-dimensional hyperbranched anatase titania architectures for high-efficiency dye-sensitized solar cells, J. Am. Chem. Soc. 136 (2014) 6437–6445. https://doi.org/10.1021/ja5015635.

[63] D.K. Roh, W.S. Chi, S.H. Ahn, H. Jeon, J.H. Kim, One-step synthesis of vertically aligned anatase thornbush-like TiO_2 nanowire arrays on transparent conducting oxides for solid-state dye-sensitized solar cells, ChemSusChem. 6 (2013) 1384–1391. https://doi.org/10.1002/cssc.201300317.

[64] H. Li, Q. Yu, Y. Huang, C. Yu, R. Li, J. Wang, F. Guo, S. Jiao, S. Gao, Y. Zhang, X. Zhang, P. Wang, L. Zhao, Ultralong Rutile TiO_2 Nanowire Arrays for Highly Efficient Dye-Sensitized Solar Cells, ACS

Appl. Mater. Interfaces. 8 (2016) 13384–13391. https://doi.org/10.1021/acsami.6b01508.

[65] S. Ni, D. Wang, F. Guo, S. Jiao, Y. Zhang, J. Wang, B. Wang, L. Yuan, L. Zhang, L. Zhao, Efficiency improvement of TiO_2 nanowire arrays based dye-sensitized solar cells through further enhancing the specific surface area, J. Cryst. Growth. 505 (2019) 62–68. https://doi.org/10.1016/j.jcrysgro.2018.09.047.

[66] J. Jiu, S. Isoda, F. Wang, M. Adachi, Dye-sensitized solar cells based on a single-crystalline TiO_2 nanorod film, J. Phys. Chem. B. 110 (2006) 2087–2092. https://doi.org/10.1021/jp055824n.

[67] L. De Marco, M. Manca, R. Giannuzzi, F. Malara, G. Melcarne, G. Ciccarella, I. Zama, R. Cingolani, G. Gigli, Novel preparation method of TiO_2-nanorod-based photoelectrodes for dye-sensitized solar cells with improved light-harvesting efficiency, J. Phys. Chem. C. 114 (2010) 4228–4236. https://doi.org/10.1021/jp910346d.

[68] W. Zhang, Y. Xie, D. Xiong, X. Zeng, Z. Li, M. Wang, Y.B. Cheng, W. Chen, K. Yan, S. Yang, TiO_2 nanorods: A facile size- and shape-tunable synthesis and effective improvement of charge collection kinetics for dye-sensitized solar cells, ACS Appl. Mater. Interfaces. 6 (2014) 9698–9704. https://doi.org/10.1021/am502067r.

[69] J. Liu, J. Luo, W. Yang, Y. Wang, L. Zhu, Y. Xu, Y. Tang, Y. Hu, C. Wang, Y. Chen, W. Shi, Synthesis of Single-Crystalline Anatase TiO_2 Nanorods with high-performance dye-sensitized solar cells, J. Mater. Sci. Technol. 31 (2015) 106–109. https://doi.org/10.1016/j.jmst.2014.07.015.

[70] B.H. Lee, M.Y. Song, S.Y. Jang, S.M. Jo, S.Y. Kwak, D.Y. Kim, Charge transport characteristics of high efficiency dye-sensitized solar cells based on electrospun TiO_2 nanorod photoelectrodes, J. Phys. Chem. C. 113 (2009) 21453–21457. https://doi.org/10.1021/jp907855x.

[71] L. Yang, W.W.F. Leung, Electrospun TiO_2 nanorods with carbon nanotubes for efficient electron collection in dye-sensitized solar cells, Adv. Mater. 25 (2013) 1792–1795. https://doi.org/10.1002/adma.201204256.

[72] X. Chen, Q. Du, W. Yang, W. Liu, Z. Miao, P. Yang, A double-layered photoanode made of ZnO/TiO_2 composite nanoflowers and TiO_2 nanorods for high efficiency dye-sensitized solar cells, J. Solid State

Electrochem. 22 (2018) 685–691. https://doi.org/10.1007/s10008-017-3806-x.

[73] M.R. Subramaniam, D. Kumaresan, S. Jothi, J.D. McGettrick, T.M. Watson, Reduced graphene oxide wrapped hierarchical TiO_2 nanorod composites for improved charge collection efficiency and carrier lifetime in dye sensitized solar cells, Appl. Surf. Sci. 428 (2018) 439–447. https://doi.org/10.1016/j.apsusc.2017.09.142.

[74] Y. Tang, C. Wang, Y. Hu, L. Huang, J. Fu, W. Yang, Preparation of anatase TiO_2 nanorods with high aspect ratio for high-performance dye-sensitized solar cells, Superlattices Microstruct. 89 (2016) 1–6. https://doi.org/10.1016/j.spmi.2015.11.003.

[75] J. Jiu, F. Wang, S. Isoda, M. Adachi, Highly efficient dye-sensitized solar cells based on single crystalline TiO_2 nanorod film, Chem. Lett. 34 (2005) 1506–1507. https://doi.org/10.1246/cl.2005.1506.

[76] S. Chatterjee, W.A. Webre, S. Patra, B. Rout, G.A. Glass, F. D'Souza, S. Chatterjee, Achievement of superior efficiency of TiO_2 nanorod-nanoparticle composite photoanode in dye sensitized solar cell, J. Alloys Compd. 826 (2020) 154188. https://doi.org/10.1016/j.jallcom.2020.154188.

[77] H.Y. Chen, T.L. Zhang, J. Fan, D. Bin Kuang, C.Y. Su, Electrospun hierarchical TiO_2 nanorods with high porosity for efficient dye-sensitized solar cells, ACS Appl. Mater. Interfaces. 5 (2013) 9205–9211. https://doi.org/10.1021/am402853q.

[78] Y. Rui, Y. Li, Q. Zhang, H. Wang, Size-tunable TiO_2 nanorod microspheres synthesised via a one-pot solvothermal method and used as the scattering layer for dye-sensitized solar cells, Nanoscale. 5 (2013) 12574–12581. https://doi.org/10.1039/c3nr04462a.

[79] S. Kathirvel, C. Su, Y.J. Shiao, Y.F. Lin, B.R. Chen, W.R. Li, Solvothermal synthesis of TiO_2 nanorods to enhance photovoltaic performance of dye-sensitized solar cells, Sol. Energy. 132 (2016) 310–320. https://doi.org/10.1016/j.solener.2016.03.025.

[80] N. Sriharan, T.S. Senthil, M. Kang, N.M. Ganesan, Rutile TiO_2 nanorod arrays incorporated with α-alumina for high efficiency dye sensitized solar cells, Appl. Phys. A Mater. Sci. Process. 125 (2019) 1–10. https://doi.org/10.1007/s00339-019-2407-1.

[81] N. Liu, X. Chen, J. Zhang, J.W. Schwank, A review on TiO_2-based nanotubes synthesized via hydrothermal method: Formation mechanism, structure modification, and photocatalytic applications, Catal. Today. 225 (2014) 34–51. https://doi.org/10.1016/j.cattod.2013.10.090.

[82] H. Cheng, Y. Feng, Y. Fu, Y. Zheng, Y. Shao, Y. Bai, Understanding and minimizing non-radiative recombination losses in perovskite light-emitting diodes, J. Mater. Chem. C. 10 (2022) 13590–13610. https://doi.org/10.1039/d2tc01869a.

[83] J. Wang, Z. Lin, Dye-sensitized TiO_2 nanotube solar cells with markedly enhanced performance via rational surface engineering, Chem. Mater. 22 (2010) 579–584. https://doi.org/10.1021/cm903164k.

[84] B.X. Lei, J.Y. Liao, R. Zhang, J. Wang, C.Y. Su, D. Bin Kuang, Ordered crystalline TiO_2 nanotube arrays on transparent FTO glass for efficient dye-sensitized solar cells, J. Phys. Chem. C. 114 (2010) 15228–15233. https://doi.org/10.1021/jp105780v.

[85] H. Park, W.R. Kim, H.T. Jeong, J.J. Lee, H.G. Kim, W.Y. Choi, Fabrication of dye-sensitized solar cells by transplanting highly ordered TiO_2 nanotube arrays, Sol. Energy Mater. Sol. Cells. 95 (2011) 184–189. https://doi.org/10.1016/j.solmat.2010.02.017.

[86] P. Roy, D. Kim, I. Paramasivam, P. Schmuki, Improved efficiency of TiO_2 nanotubes in dye sensitized solar cells by decoration with TiO_2 nanoparticles, Electrochem. Commun. 11 (2009) 1001–1004. https://doi.org/10.1016/j.elecom.2009.02.049.

[87] Z. He, W. Que, P. Sun, J. Ren, Double-layer electrode based on TiO_2 nanotubes arrays for enhancing photovoltaic properties in dye-sensitized solar cells, ACS Appl. Mater. Interfaces. 5 (2013) 12779–12783. https://doi.org/10.1021/am4044745.

[88] N. Fu, X. Jiang, D. Chen, Y. Duan, G. Zhang, M. Chang, Y. Fang, Y. Lin, Au/TiO_2 nanotube array based multi-hierarchical architecture for highly efficient dye-sensitized solar cells, J. Power Sources. 439 (2019) 227076. https://doi.org/10.1016/j.jpowsour.2019.227076.

[89] B. Bozkurt Çırak, Ç. Eden, Y. Erdoğan, Z. Demir, K.V. Özdokur, B. Caglar, S. Morkoç Karadeniz, T. Kılınç, A. Ercan Ekinci, Ç. Çırak, The enhanced light harvesting performance of dye-sensitized solar cells based on ZnO nanorod-TiO_2 nanotube hybrid photoanodes, Optik (Stuttg). 203 (2020).

https://doi.org/10.1016/j.ijleo.2019.163963.

[90] W.Q. Wu, Y.F. Xu, H.S. Rao, C.Y. Su, D. Bin Kuang, Trilayered photoanode of TiO_2 nanoparticles on a 1D-3D nanostructured TiO_2-grown flexible Ti substrate for high-efficiency (9.1%) dye-sensitized solar cells with unprecedentedly high photocurrent density, J. Phys. Chem. C. 118 (2014) 16426–16432. https://doi.org/10.1021/jp4116782.

[91] M. Abdullah, S.K. Kamarudin, Titanium dioxide nanotubes (TNT) in energy and environmental applications: An overview, Renew. Sustain. Energy Rev. 76 (2017) 212–225. https://doi.org/10.1016/j.rser.2017.01.057.

[92] M. Adachi, Y. Murata, I. Okada, S. Yoshikawa, Formation of Titania Nanotubes and Applications for Dye-Sensitized Solar Cells, J. Electrochem. Soc. 150 (2003) G488. https://doi.org/10.1149/1.1589763.

[93] Q. Zheng, H. Kang, J. Yun, J. Lee, J.H. Park, S. Baik, Hierarchical construction of self-standing anodized titania nanotube arrays and nanoparticles for efficient and cost-effective front-illuminated dye-sensitized solar cells, ACS Nano. 5 (2011) 5088–5093. https://doi.org/10.1021/nn201169u.

[94] J.H. Hu, S.Q. Tong, Y.P. Yang, J.J. Cheng, L. Zhao, J.X. Duan, A composite photoanode based on P25/TiO_2 nanotube arrays/flower-like TiO_2 for high-efficiency dye-sensitized solar cells, Acta Metall. Sin. (English Lett. 29 (2016) 840–847. https://doi.org/10.1007/s40195-016-0460-8.

[95] J. Khan, J. Gu, S. He, X. Li, G. Ahmed, Z. Liu, M.N. Akhtar, W. Mai, M. Wu, Rational design of a tripartite-layered TiO_2 photoelectrode: A candidate for enhanced power conversion efficiency in dye sensitized solar cells, Nanoscale. 9 (2017) 9913–9920. https://doi.org/10.1039/c7nr03134c.

[96] W. Zhu, Y. Liu, A. Yi, M. Zhu, W. Li, N. Fu, Facile fabrication of open-ended TiO_2 nanotube arrays with large area for efficient dye-sensitized solar cells, Electrochim. Acta. 299 (2019) 339–345. https://doi.org/10.1016/j.electacta.2019.01.021.

[97] H. Wang, M. Liu, M. Zhang, P. Wang, H. Miura, Y. Cheng, J. Bell, Kinetics of electron recombination of dye-sensitized solar cells based on TiO_2 nanorod arrays sensitized with different dyes, Phys. Chem. Chem. Phys. 13 (2011) 17359–17366. https://doi.org/10.1039/c1cp22482d.

[98] M. Yang, D. Kim, H. Jha, K. Lee, J. Paul, P. Schmuki, Nb doping of TiO_2 nanotubes for an enhanced

efficiency of dye-sensitized solar cells, Chem. Commun. 47 (2011) 2032–2034. https://doi.org/10.1039/c0cc04993j.

[99] S. So, K. Lee, P. Schmuki, Ru-doped TiO_2 nanotubes: Improved performance in dye-sensitized solar cells, Phys. Status Solidi - Rapid Res. Lett. 6 (2012) 169–171. https://doi.org/10.1002/pssr.201105600.

[100] L. De Marco, M. Manca, R. Giannuzzi, M.R. Belviso, P.D. Cozzoli, G. Gigli, Shape-tailored TiO_2 nanocrystals with synergic peculiarities as building blocks for highly efficient multi-stack dye solar cells, Energy Environ. Sci. 6 (2013) 1791–1795. https://doi.org/10.1039/c3ee24345a.

[101] K. Lee, A. Mazare, P. Schmuki, One-dimensional titanium dioxide nanomaterials: Nanotubes, Chem. Rev. 114 (2014) 9385–9454. https://doi.org/10.1021/cr500061m.

[102] A. Soussi, A. Ait Hssi, M. Boujnah, L. Boulkadat, K. Abouabassi, A. Asbayou, A. Elfanaoui, R. Markazi, A. Ihlal, K. Bouabid, Electronic and Optical Properties of TiO_2 Thin Films: Combined Experimental and Theoretical Study, J. Electron. Mater. 50 (2021) 4497–4510. https://doi.org/10.1007/s11664-021-08976-8.

[103] Y.M. Evtushenko, S. V. Romashkin, N.S. Trofimov, T.K. Chekhlova, Optical Properties of TiO_2 Thin Films, Phys. Procedia. 73 (2015) 100–107. https://doi.org/10.1016/j.phpro.2015.09.128.

[104] M.I. Khan, K.A. Bhatti, R. Qindeel, H.S. Althobaiti, N. Alonizan, Structural, electrical and optical properties of multilayer TiO_2 thin films deposited by sol–gel spin coating, Results Phys. 7 (2017) 1437–1439. https://doi.org/10.1016/j.rinp.2017.03.023.

[105] R. Qian, H. Zong, J. Schneider, G. Zhou, T. Zhao, Y. Li, J. Yang, D.W. Bahnemann, J.H. Pan, Charge carrier trapping, recombination and transfer during TiO_2 photocatalysis: An overview, Catal. Today. 335 (2019) 78–90. https://doi.org/10.1016/j.cattod.2018.10.053.

[106] F. Yang, J. Xi, L.Y. Gan, Y. Wang, S. Lu, W. Ma, F. Cai, Y. Zhang, C. Cheng, Y. Zhao, Improved charge transfer and photoelectrochemical performance of $CuI/Sb_2S_3/TiO_2$ heterostructure nanotube arrays, J. Colloid Interface Sci. 464 (2016) 1–9. https://doi.org/10.1016/j.jcis.2015.11.004.

[107] A. Al Mayyahi, B.M. Everhart, T.B. Shrestha, T.C. Back, P.B. Amama, Enhanced charge separation in TiO_2/nanocarbon hybrid photocatalysts through coupling with short carbon nanotubes, RSC Adv.

11 (2021) 11702–11713. https://doi.org/10.1039/d1ra00045d.

[108] P. Wadhwa, S. Kumar, T.J.D. Kumar, A. Shukla, R. Kumar, Bandgap tunability in a one-dimensional system, Condens. Matter. 3 (2018) 1–10. https://doi.org/10.3390/condmat3040034.

[109] S. Singh Surah, M. Vishwakarma, R. Kumar, R. Nain, S. Sirohi, G. Kumar, Tuning the electronic band alignment properties of TiO_2 nanotubes by boron doping, Results Phys. 12 (2019) 1725–1731. https://doi.org/10.1016/j.rinp.2019.01.081.

[110] B. Minhas, S. Dino, H. Qian, Y. Zuo, An approach for high stability TiO_2 in strong acid environments at high temperature, Surf. Coatings Technol. 395 (2020) 125932. https://doi.org/10.1016/j.surfcoat.2020.125932.

[111] D.J. Mowbray, J.I. Martinez, G.J.M. Lastra, K.S. Thygesen, K.W. Jacobsen, Stability and electronic properties of TiO_2 nanostructures with and without b and n doping, J. Phys. Chem. C. 113 (2009) 12301–12308. https://doi.org/10.1021/jp904672p.

[112] P.K. Das, A.K. Mallik, A.H. Molla, A.K. Santra, R. Ganguly, A. Saha, S. Kumar, V.K. Aswal, Experimental investigation for stability and surface properties of TiO_2 and Al_2O_3 water-based nanofluids, J. Therm. Anal. Calorim. 147 (2022) 5617–5635. https://doi.org/10.1007/s10973-021-10894-0.

[113] S.C. Poh, H. Ahmad, C.H. Ting, H.T. Tung, H.K. Jun, Performances of flexible dye-sensitized solar cells fabricated with binder-free nanostructure TiO_2, J. Mater. Sci. Mater. Electron. 32 (2021) 12031–12041. https://doi.org/10.1007/s10854-021-05833-6.